

Review

Amygdaloid complex anatomopathological findings in animal models of *status epilepticus*

Cristiane Queixa Tilelli ^{a,*}, Larissa Ribeiro Flôres ^a, Vinicius Rosa Cota ^b,
Olagide Wagner de Castro ^c, Norberto Garcia-Cairasco ^{d,*}

^a Laboratory of Physiology, Campus Centro-Oeste Dona Lindu, Universidade Federal de São João del-Rei, Av. Sebastião Gonçalves Coelho, 400, Bairro Belvedere, Divinópolis, MG 35.501-296, Brazil

^b Laboratory of Neuroengineering and Neuroscience (LINNce), Department of Electrical Engineering, Campus Santo Antônio, Universidade Federal de São João del-Rei, Praça Frei Orlando, 170, Centro, São João Del Rei, MG 36307-352, Brazil

^c Institute of Biological Sciences and Health, Campus A. C. Simões, Universidade Federal de Alagoas, Av. Louival Melo Mota, s/n, Tabuleiro do Martins, Maceió, AL 57072-970, Brazil

^d Neurophysiology and Experimental Neuroethology Laboratory (LNNE), Department of Physiology, School of Medicine, Universidade de São Paulo, Av. Bandeirantes, 3900, Monte Alegre, Ribeirão Preto, SP 14049-900, Brazil

ARTICLE INFO

Article history:

Received 11 July 2019

Revised 15 November 2019

Accepted 25 November 2019

Available online 19 December 2019

Keywords:

Epilepsy

Amygdaloid complex

Status epilepticus

Plasticity

ABSTRACT

Temporal lobe epileptic seizures are one of the most common and well-characterized types of epilepsies. The current knowledge on the pathology of temporal lobe epilepsy relies strongly on studies of epileptogenesis caused by experimentally induced *status epilepticus* (SE). Although several temporal lobe structures have been implicated in the epileptogenic process, the hippocampal formation is the temporal lobe structure studied in the greatest amount and detail. However, studies in human patients and animal models of temporal lobe epilepsy indicate that the amygdaloid complex can be also an important seizure generator, and several pathological processes have been shown in the amygdala during epileptogenesis.

Therefore, in the present review, we systematically selected, organized, described, and analyzed the current knowledge on anatomopathological data associated with the amygdaloid complex during SE-induced epileptogenesis. Amygdaloid complex participation in the epileptogenic process is evidenced, among others, by alterations in energy metabolism, circulatory, and fluid regulation, neurotransmission, immediate early genes expression, tissue damage, cell suffering, inflammation, and neuroprotection. We conclude that major efforts should be made in order to include the amygdaloid complex as an important target area for evaluation in future research on SE-induced epileptogenesis.

This article is part of the Special Issue "NEWscience 2018".

© 2019 Elsevier Inc. All rights reserved.

1. Introduction

Epilepsy is one of the most common neurological conditions in the world, affecting all ages, ethnicities, and social classes, imposing a major burden in psychological, physical, social, and economic areas [1–3]. Worldwide, it is estimated that about 85 million people live with epilepsy, and its annual incidence reaches 61.4 per 100,000 inhabitants [4].

Epileptic seizures are transitory electrophysiological events characterized by synchronous and excessive neuronal activity in the brain [5]. They are accompanied by abnormal, subtle, and transitory alterations of consciousness and/or motor, sensitive, autonomic, or psychic symptoms, perceived by the patient or an observer [6]. The process by which pathological alterations gradually occur in the brain, leading a

previously normal neural network to evolve to an epileptic one is referred to as epileptogenesis [7–9]. Temporal lobe structures, such as the hippocampus, the amygdaloid complex, and the pyriform cortex, when lesioned, are some of the most susceptible regions to the maladaptive epileptogenic plasticity [7,10].

The epileptogenic process is studied preclinically mostly utilizing rodents as subjects, divided in two groups of experimental models [11–14]. In the now classical kindling model, repeated subthreshold electrical stimuli result in progressive behavioral and electrographic (electroencephalogram (EEG)) epileptiform response, leading to the consistent occurrence of stimulus-induced generalized seizures [8,13,15,16]. Epileptogenesis can also be induced in animals that are submitted to *status epilepticus* (SE), an abnormally prolonged seizure that occurs after a single insult [10,13,17–19]. Convulsive SE can endure several hours, depending on the chosen post-SE treatment protocol and SE refractoriness to medication [14,19]. SE is followed by a latent period, when several neuroplastic alterations occur in the brain while no

* Corresponding authors.

E-mail addresses: c.tilelli@uol.com.br (C.Q. Tilelli), ngcairasco@usp.br (N. Garcia-Cairasco).

seizures are observed [10,13]. In animal models, one to two weeks after SE, the chronic stage starts, characterized by the presence of spontaneous recurrent seizures [10,13].

A great number of studies using animal models of SE focus on pathological alterations in the hippocampus as the main area involved in epileptogenesis [20–22]. Nonetheless, many other studies implicate the amygdaloid complex in seizure generation, seizure activity, and epileptogenesis [15,23–29]. For example, inflammatory processes related to seizures evolve jointly or even faster in the amygdala, when compared with the hippocampus [30,31]. Furthermore, electrode implantation in the amygdala alone increases epileptogenesis [32]. Interictal epileptic discharges tend to be initiated in the amygdala or in the nearby cortical areas, such as the piriform cortex [23,24,33,34]. Additionally, in most of the cases, patients with epilepsy submitted to surgical ablation of the temporal lobe can only obtain full control of seizures if the amygdala is also resected [35]. Occasionally, removal of only the amygdala is enough to decrease seizures [36].

The amygdaloid complex modulates cognitive functions and plays a central role in the processing of emotional memories, emotionally driven behaviors, and mood/affective perturbations [37]. Furthermore, it presents rich network connections with other temporal lobe structures [38]. Consequently, the epilepsies involving this area are important not only for their role in specific kinds of seizures but also in the expression of psychiatric comorbidities that are associated with this disease [39].

The amygdala participation and importance in temporal lobe epilepsy and its comorbidities have been reviewed, most recently with focus on emotional disturbances, electrophysiological phenomena, computational network analysis, and pathophysiology [40–43]. Conversely, there has been no recent structured and comprehensive review on amygdala pathology in animal models of SE. We believe that the summarized data from the literature allow an increased perception on the amygdala participation in epileptogenesis, providing opportunities to formulate new hypothesis, discuss about diverging and convergent views, and draw new perspectives and insights.

2. Methods

A search in PubMed Medline® database was performed using the following terms, without any date restriction: ("status epilepticus"[MeSH Terms] OR "status epilepticus"[All Fields]) AND ("amygdala"[MeSH Terms] OR "amygdala"[All Fields] OR "amygdaloid complex"[All Fields]) AND ("pilocarpine"[MeSH Terms] OR "pilocarpine"[All Fields]) OR ("kainic acid"[MeSH Terms] OR "kainic acid"[All Fields]) OR ("electric stimulation"[MeSH Terms] OR "electric stimulation"[All Fields] OR "electrical stimulation"[All Fields]) AND ("rats"[MeSH Terms] OR "rats"[All Fields] OR "rat"[All Fields]).

Only articles written in English that used young adult and/or adult male rats with SE induced by electrical or chemical stimulation were used. The articles should describe amygdala alterations during or consequent to SE. Publications based on protocols that induced direct mechanical, chemical, or electrical damage to the amygdala were excluded. Other criteria for exclusion were lack of appropriate controls for the purpose of this review (sham/vehicle-treated animals), inclusion of areas adjacent to the amygdala in evaluations, and diverging data/conditions described. Some types of articles were not included: review articles, articles that were based on human studies only, those that did not use rats or used only modified rat strains, and those that did not show anatomopathological or related findings. Additionally, female (young and adult) and young (male and female) rats were not included, given that such animals have specific modifying factors to be considered, such as hormonal cycle influences and central nervous system developmental processes [44–49]. Subsequent searches were performed in order to verify the addition of new publications between the first list of publications and the finalization of this review (last search date was June, 2019).

Research papers were selected or excluded based on three phases. In the first phase, we excluded only those articles that could be ruled out undoubtedly by their Abstracts. If any uncertainty remained, the article was left to the second phase. In this phase, all articles that remained were read entirely, and the decision was taken for their maintenance or not in the review. Two authors (CQT and LRF) evaluated all Abstracts (first phase) and papers (second phase) and decided if they would be included in the current review. In the third phase, all the relevant information was collected: age and strain of the rats, method for SE induction and termination, duration of SE, and main anatomopathological results presented.

3. Results

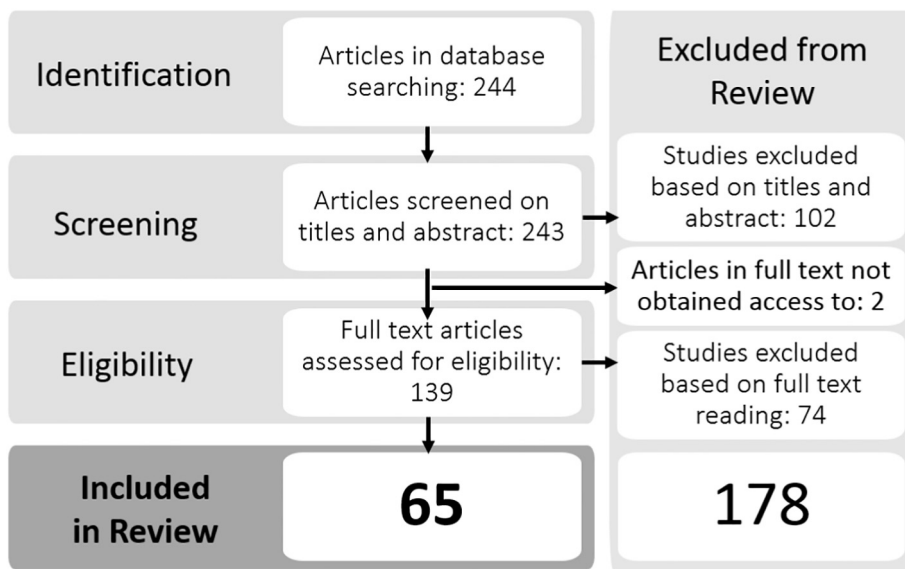
3.1. Publications included in the review: general characterization

The sequence of procedures for the selection process of the articles to be included in this study is presented in Fig. 1. The oldest article found in the search was from 1975. The total number of articles screened was 243. One hundred and two (102) did not reach inclusion criteria during the first phase (screening by Title and Abstract reading), leaving 141 to be completely read. We did not obtain access to 2 articles, so they were excluded as well. After complete reading, another 74 articles were excluded from this review. Therefore, in total, 178 articles were excluded from the review, and 65 articles were considered adequate for our study. All references in the final search are divided in 2 tables: Table 1, with the articles included in the review and their main data, and the Supplemental Table, where the articles excluded from the review are listed with the reason for their exclusion.

Articles included in the review were published between 1983 and 2018. The majority of them presented data from SE induced by systemic injections of pilocarpine or kainic acid (55 publications). SE could also be induced systemically by soman or MK-801 followed by pilocarpine injections, or locally by kainic acid or carbachol injections, or by electrical stimulation of limbic areas outside the amygdaloid complex. We classified each data according to the following categories: energy metabolism-, neuroprotection-, circulatory and fluid regulation-, neurotransmission-, immediate early genes-, tissue damage-, inflammation-, plasticity-, and cell suffering-related data. Using the classified data from Table 1, it was possible to create a timeline or kinetics with the main anatomopathological processes identified in the amygdaloid complex after SE in young adult and adult male rats (Fig. 2).

3.2. Current literature on amygdaloid complex anatomopathological processes after SE: detailed description

Brain regional metabolism quantification during seizures and interictal periods can be used to identify the nervous system structures responsible for the generation, maintenance, propagation, and control of the epileptic activity [112,113]. Once SE is initiated, the first alterations observed in the amygdala are metabolic. There is an immediate (3 min) increase, followed by a decrease (15–120 min), in brain perfusion rate (BPR) and in the apparent diffusion coefficient (ADC) signal [62–64]. Regardless of the behavioral and electrographic differences in SE observed between animals [28,29], those initial alterations are accompanied by an increase in local glucose uptake [28,29,84,97,110]. High-energy phosphates (adenosine triphosphate, phosphocreatine) are reduced in about 50% 1–2 h after SE onset [69,70], suggesting that the increased glucose uptake is not sufficient to provide the amount of energy demanded by the amygdala during SE. Blood-brain barrier leak starts, especially in the medial amygdaloid nucleus [80]. Subsequently, at 24 h after SE, vascular endothelial growth factor (VEGF) is increased [87], possibly as an attempt to compensate the increased demand for energy. In fact, 14 days after SE, the blood vessel density is increased in the amygdala [73]. On the other hand, during the first 2 h of SE, morphology shown by magnetic resonance images (MRI) is normal, neuronal

**Fig. 1.** Flowchart of the articles' selection process.

survival is maintained, and most cell damage and inflammation markers are sparsely or not observed [62,67,79,85,86,92,96,103,108].

The genomic reprogramming in response to the damage caused by SE includes the expression of hundreds of genes, and this is coincident with the distribution map of Fos protein expression [60,84]. Fos is one of the most reported immediate early genes that are expressed after an epileptic seizure, activated because of excessive neuronal activity [114–116]. Immediate early genes start to appear 2 h after SE onset (and after SE termination, depending on the study), in several amygdaloid nuclei [52,60,74,84,90]. Fos and Fos B proteins are expressed in superposing time points after SE. Fos-positive strongest immunoreactions are observed 2–4 h after SE, while Fos B protein expression peak occurs up to 2 days later [90]. Nonetheless, they can be both observed concomitantly between 2 and 24 h after SE in the medial amygdaloid nucleus after SE [60,90]. Other immediate early genes-positive (jun D proto-oncogene and c-jun) neurons are increased as well [59,60]. All the above phenomena are described in the first minutes to hours after SE, indicating a great amount of activity in the amygdala and related areas. Conversely, one study showed that there are no alterations in dopamine and catecholamine metabolites' levels in the amygdala 30 min after SE onset [50]. Glucose uptake remains increased for several hours as compared with the baseline [28,98,99]. However, the high-energy phosphates are maintained in lower levels in the amygdala up to 3 days after SE [70].

Several studies have also shown that the later appearance of neuronal lesions in the amygdala can be directly associated with local hypermetabolism and increased T2-weighted signal intensity in the MRI during the first minutes to hours after SE onset [28,61,65,92,96]. Correspondingly, as early as 2.5 h after SE induced by pilocarpine (but not by kainic acid), some silver-impregnated neurons are seen in the amygdala [56]. On the other hand, inflammatory process markers and gliosis were not seen before 4–12 h after SE [79,81,86,92,103,111]. Epileptic seizures can increase the expression of inflammatory mediators in the brain regions involved in the generation and in the propagation of epileptic activity [117–120].

Neuronal damage is evident in the amygdala starting 4 h and peaking 12–48 h after SE [56,57,108,111,74,75,79,81,86,92,94,100]. Markers of inflammation and oxidative stress such as histamine, caspase 3, and cytochrome c oxidase activity present a similar pattern [81,86,94,108,111]. In addition, microglia activation, gliosis, and tissue edema are also observed [56,57,75,86,92].

An increase in citrulline, a determinant of nitric oxide presence in the tissue, is observed in the amygdala at this time [70]. Accordingly,

cyclooxygenase-2, an enzyme that may be induced by nitric oxide, start to rise in several amygdaloid nuclei as well: lateral, basolateral, basomedial, and cortical [74]. In the lateral nucleus of the amygdala, there is an increase in the number of neurons immunoreactive to the proapoptotic B-cell lymphoma 2-associated X (Bax) protein, while no alterations are observed for the antiapoptotic protein B-cell lymphoma 2 (Bcl2) [103]. The underlying damage process in the amygdala also starts to be more evident about 12–24 h after SE in MRI studies. This is observed by an initial decrease in T2-weighted signal, with peak at 24–72 h after SE [61,65,92,95,96,101,105].

While peaks in neuronal damage occur between 8 and 48 h after SE, the degenerating process is progressive and lasts several weeks to months in the amygdala. The degeneration is shown through the observation of pyknotic neurons, FluoroJade-positive neurons [121,122], and neurons with deoxyribonucleic acid fragmentation [56,71,86,93,103,104,108]. Likewise, the amygdaloid complex showed reduced cell counts using thionin or immunohistochemistry for neuronal markers such as the neuronal nuclei protein Neu-N, microtubule-associated protein 2 (MAP2), and glutamic acid decarboxylase (GAD) [17,54,67,68,71,75–79,81,86,56,92,93,96,99,102–104,106,108,109,58,59,61,62,64–66]. Some amygdaloid nuclei such as the lateral, basal, medial, and cortical, are more prone to damage than others, for example, the dorsal lateral and the central amygdaloid nuclei [58,71,92,103,104].

Two to three weeks after SE, positive silver staining or argyrophilic neurons, known to be neurons in distress, are present in the amygdala [71,93,104]. Concomitantly, cell reorganization with synaptic plasticity are also part of the observed consequences to SE in the amygdala. Newly generated cells are detected and are later (42 days after SE) observed with neuronal or glial phenotypes [75]. Interestingly, such cells do not migrate from other areas but are generated locally [75]. Additionally, during this same time range, the metabotropic glutamate receptor mGluR5 availability and zinc-containing fibers (Timm staining) are not altered or reduced [53,55,89]. Likewise, histamine receptors H1 and H3 binding and messenger ribonucleic acid (mRNA) expression decrease [81]. On the other hand, other molecules are increased, such as histamine and histamine-reactive fibers, the gamma-aminobutyric acid (GABA) transporters GAT-1 and GAT-3, neuropeptide Y immunoreactive neurons, mu-opioid receptors binding, microtubule-associated protein-2 (MAP2), stromal-derived factor 1 alpha (SDF-1 alpha), and synaptophysin [72,75,81,83,89,91,100]. The SDF-1 alpha and synaptophysin hyperregulation suggests cell synthesis, migration, and synaptic remodeling in the amygdaloid complex circuitry [72,123]. Furthermore, the increased expression of GAT-1 and GAT-3 suggests a

Table 1

Publications included in the review and main data collected (total 65).

Authors	SE induction method; SE duration	Data
Alam and Starr, 1996 [50]	Systemic lithium + pilocarpine or intrahippocampal carbachol; 30 min	■ 30 min after self-sustained SE started: no alteration in dopamine, DOPAC (dopamine metabolite) and HVA (catecholamine metabolite) levels (HPLC).
Atanasova et al., 2018 [51]	Systemic kainic acid; at least 3 h	■ 5 months: reduced angiotensin II receptor (type 1; AT1) expression at the temporal part of the basolateral amygdala.
Barone et al., 1993 [52]	Systemic pilocarpine; 2–4 h	■ 2–4 h: positive Fos staining, especially in the basolateral nucleus
Cavarsan et al., 2012 [53]	Systemic methyl-scopolamine + pilocarpine; 90–150 min	■ 2 and 8 h, 1 and 7 days: increased Homer1a with peak at 24 h; mGluR5 not different from control
Chen and Buckmaster, 2005 [54]	Systemic kainic acid; at least 4 h	■ 7–12 months after SE: reduced amygdaloid complex volume, especially posterior portions
Choi et al., 2014 [55]	Systemic lithium + methyl-scopolamine + pilocarpine; at least 1 h	■ 24 h and 7 days after SE: mGluR5 availability is reduced, peak at 7 days (measured by ^{[11]C} JABP688 positron emission tomography tracer)
Covolan and Mello, 2000 [56]	Systemic methyl-scopolamine + pilocarpine or kainic acid; at least 90 min	■ 4 weeks after SE: mGluR5 binding potential back to control levels
Dedeurwaerdere et al., 2012 [57]	Systemic kainic acid; at least 4 h	■ 2.5 h: some silver-impregnated neurons are seen in the amygdala of pilocarpine-injected animals but not KA-injected animals.
Dos Santos et al., 2005 [58]	Systemic methyl-scopolamine + pilocarpine; at least 90 min	■ 8 h: peak of silver-impregnated neurons in several amygdaloid nuclei (basolateral, anterior, basomedial, central, cortical, lateral), in both models;
Dragunow et al., 1993 [59]	Dorsal hippocampus electrical stimulation or MK801 + pilocarpine; "many hours"	■ 8–48 h: edema, with peak at 24 h, especially in the cortical nucleus
Dube et al., 1998 [60]	Systemic lithium + methyl-scopolamine + pilocarpine; at least 2 h	■ 7 days after SE: translocator protein and OX42 (markers of activated microglia) increased in the amygdala, higher in more severe SE.
Ebisu et al., 1994 [61]	Systemic kainic acid; 4–8 h	■ About 60 days after SE: reduced volume of the central amygdaloid nucleus; no reduction in the lateral and basolateral nuclei; Sprouting (NeuN staining) reduced in the central amygdaloid nucleus and not altered in the lateral and basolateral amygdaloid nuclei
Engelhorn et al., 2005 [62]	Systemic methyl-scopolamine + pilocarpine; up to 8 h	■ 24 h: c-Jun mRNA and protein expressed in the amygdala
Engelhorn, Hufnagel, et al., 2007 [63]	Systemic methyl-scopolamine + pilocarpine; SE duration not informed	■ 6 days: cell loss in the amygdala
Engelhorn, Weise, et al., 2007 [64]	Systemic methyl-scopolamine + pilocarpine; up to 8 h	■ 2 and 24 h after SE: high Fos staining ("early" and "late" waves, respectively)
Fabene et al., 2003 [65]	Systemic methyl-scopolamine + pilocarpine; at least 4 h	■ 6 h after SE: high density of silver-stained neurons;
Figueiredo et al., 2011 [66]	Systemic hydroxyiminomethyl-pyridinium + soman + atropine; about 10 h	■ 24 h after SE: Jun-D moderately induced, low to moderate levels of HSP70;
Francois et al., 2011 [67]	Systemic lithium + methyl-scopolamine + pilocarpine; SE duration not informed	■ 2 days after SE: no Fos was observed in the amygdala
Fritsch et al., 2009 [68]	Systemic kainic acid; at least 3 h	■ 3 days: reduced levels of N-acetyl-aspartate (MRI), high T2 signal intensity and high degree of cell loss; there was correlation between the parameters.
Gupta and Dettbarn, 2003 [69]	Systemic kainic acid; at least 1 h	■ 3 min after SE onset: brain perfusion rate increased ($129 \pm 16\%$);
Gupta et al., 2000 [70]	Systemic kainic acid; SE duration not informed	■ 15, 30, 60, and 120 min after SE onset: brain perfusion rate reduced (maximal at 60 min, 62% from baseline);
Halonen, Nissinen and Pitkänen, 1999 [71]	Perforant path electrical stimulation; 40–60 min	■ 0.5 and 2 h after SE onset: no difference in surviving neurons
Hanaya, Boehm and Nehlig, 2007 [72]	Systemic lithium + methyl-scopolamine + pilocarpine; 6–8 h	■ 24 h, 1, and 2 weeks: progressively reduced percentage of surviving neurons in the amygdala, 66, 54, and 38%, respectively.
Handforth and Ackermann, 1995 [29]	Electrical stimulation of several brain areas; 40–50 min	■ 3, 5, 10, 15, 20, 30, 45, 60, 90, and 120 min apparent diffusion coefficient: peak increase at 3 min after seizure onset and reduced from 15 to 120 min (peak 30–90 min); no differences were observed 5 and 10 min after seizure onset.
		■ 0.5, 2 h, 1, 7, 14 days: progressively reduced surviving neurons from 1 day to 14 days, reaching 38% from control (62% reduction).
		■ 3 min after seizure onset: increased apparent diffusion coefficient;
		■ 30, 60, 90, and 120 min after seizure onset: reduced apparent diffusion coefficient;
		■ 5, 10, and 15 min after seizure onset: no alterations in apparent diffusion coefficient;
		■ 2 weeks after SE: 38% surviving cells in the amygdala
		■ 12 h after SE: reduction of apparent diffusion coefficient (61%); increased T2-weighted MRI (22%); "numerous" FluoroJade B-positive neurons in the amygdala.
		■ 1 and 7 days after SE: basolateral amygdala evaluated; 64% neuronal survival, score moderate for neurodegeneration (FluoroJade C staining); GABAergic neurons (GAD67) were not different at 1 day after SE but were reduced at 7 days after SE, in the same proportion of general neuronal loss.
		■ 0.5, 3, 8, and 24 h: FluoroJade B staining progressively increased with statistical significance at 24 h.
		■ 14 days: basolateral amygdala 72% and median nucleus 38–52% neuronal loss.
		■ 7–10 days after SE: 15% reduction in total neuron and 43% reduction in GAD67 neurons (special vulnerability of inhibitory neurons in the amygdala); FluoroJade C-positive cells (basolateral, medial, lateral, posterior cortical, central amygdala nuclei); increased GAD65–67 protein in the amygdala ($27.1 \pm 7.8\%$); GABA _A subunit alpha1 also increased ($157 \pm 19\%$); glutamate receptor GluK1 reduced to $73.0 \pm 4.6\%$ of control group.
		■ 2 h after KA injection: increased citrulline (300%); and decreased high-energy phosphates (55%, adenosine triphosphate, total adenine nucleotides, nicotinamide adenine dinucleotide, phosphocreatine, and total creatine compounds).
		■ 1 h and 3 days: high-energy phosphates – adenosine triphosphate, total adenine nucleotides (ATP + ADP + AMP), phosphocreatine and total creatine compounds (phosphocreatine + creatine) – reduced in about 50%.
		■ 2 weeks after SE induction: neuronal damage observed in 15 of 18 amygdaloid areas evaluated (silver staining). Especially damaged: lateral, basal, and cortical nuclei.
		■ 1, 3, 7, and 21 days after SE: increased synaptophysin expression, peak at 1 day, tending back to normal, statistical significance lost at 7 days; GAP-43: reduced in all amygdala areas (laterodorsal, basolateral, centrolateral, medial), starting at 7 days and reducing more at 21 days
		■ Detailed study, based on behavior and EEG, different types of SE were suggested; 40–50 min after self-sustained SE started: amygdala was involved in all patterns of SE obtained in the experiments (¹⁴ C-2DG, slice radiography).

Table 1 (continued)

Authors	SE induction method; SE duration	Data
Handforth and Treiman, 1995 [28]	Systemic lithium + pilocarpine; 1–2 h	<ul style="list-style-type: none"> ■ Detailed SE study based on EEG; different stages of SE were determined; increased signal in the amygdala in all stages evaluated (¹⁴C-2DG, slice radiography)
Hayward et al., 2010 [73]	Systemic scopolamine + pilocarpine; SE duration was not informed	<ul style="list-style-type: none"> ■ 2 and 14 days after SE: no alterations in cerebral blood volume; increased cerebral blood flow in the amygdala at 2 (16%) and 14 (30%) days; at 14 days, 27% increase in blood vessel density in the amygdala.
Joseph et al., 2006 [74]	Systemic dextrose + kainic acid; 4–5 h	<ul style="list-style-type: none"> ■ 2, 6, 24 h: increased COX-2 in neurons at all time points, peak at 24 h (amygdala nuclei marked: lateral, basolateral, basomedial, and posterolateral cortical); ■ 2 h: Fos staining in several nuclei of the amygdala
Jung et al., 2009 [75]	Systemic lithium + methyl-scopolamine + pilocarpine; at least 1 h	<ul style="list-style-type: none"> ■ 14 and 42 days after SE: 33% reduction in cell number in the amygdala; increased OX-42 (microglial activation marker), peak at 14 days; same pattern for proliferation (BrdU); at 42 days, newly generated cells were 20% neurons, 30% astrocytes, and 25% oligodendrocytes (at 42 days) ■ 1, 3, and 28 d: SDF-1a prominently increased in the amygdala, mainly astrocytes. ■ 6–7 weeks after SE: moderate to severe damage (medial division of the lateral nucleus, periamygdaloid cortex, posterior cortical nucleus, lateral division of amygdalohippocampal area); mild to moderate damage (lateral part of parvcellular division of the basal nucleus, accessory basal nucleus, anterior cortical nucleus, other areas of periamygdaloid cortex, medial division of amygdalohippocampal area). Reduced retrograde labeling of amygdala neurons by tracers injected in hippocampus. ■ 13–15 weeks after SE: the lateral nucleus of the amygdala was evaluated; dorsolateral division not affected; ventrolateral and medial divisions presented positive damage score (as compared with zero in control rats) and volume reduction of up to 23% from control.
Kemppainen and Pitkänen, 2004 [76]	Systemic kainic acid; SE duration not informed	<ul style="list-style-type: none"> ■ 21 days after SE: all animals with 90 min or longer SE duration presented necrosis in the amygdala; 3/9 and 9/17 animals presented necrosis in the amygdala after 7.5- and 15-min SE duration, respectively.
Kemppainen, Nissinen and Pitkänen, 2006 [77]	Systemic kainic acid; SE duration not informed	<ul style="list-style-type: none"> ■ 1 and 3 h after SE onset: no difference in IL-6 or glycoprotein 130 (GP130) expression relative to control. ■ 6 and 12 h after SE onset: increased IL-6 expression; GP130 expression continues at normal levels. ■ 1 and 3 d after SE onset: no difference in IL-6 or GP130 expression relative to control. ■ 7 days after SE onset: no difference in IL-6 expression relative to control; GP130 hyperregulation. ■ 90 min after SE onset: blood–brain barrier leak in the medial (66%), but not in the basolateral, amygdaloid nucleus; increased cerebral blood volume (generalized); ■ 2 months after SE: reduced cell count in the medial amygdaloid nucleus ■ Histamine H1 receptor mRNA expression after SE: not altered at 3 and 6 h; reduced expression levels at 12 h, 1, 2, 3, and 7 days; back to normal levels at 4 weeks, 6 months, and 1 year. ■ Histamine H1 receptor binding after SE: not altered at 3, 6, and 12 h; reduced at 1, 2, 3, and 7 days; back to normal levels at 6 months and 1 year. ■ Histamine H3 receptor mRNA expression after SE: not altered at 3 and 6 h; variable at 12 h (depending on the isoform); reduced at 1, 2, and 3 days; isoforms return to normal levels between 7 days and 4 weeks and maintain in normal levels 6–12 months. ■ Histamine H3 receptor binding after SE: not altered at 3, 6, and 12 h; reduced at 1, 2, 3, 7 days, 4 weeks, 6 months, and 1 year. ■ Histamine levels (HPLC): increased at 6 h, 1, 3, 7 days. ■ Histamine-reactive fibers: increased at 6 h, 1, 2, 3 days, 4 weeks; back to normal levels 1 year after SE. ■ 13 weeks after SE: reduced protein phosphatase 2A activity; reduced expression of its regulatory B unit PR55; increased ratio of phosphorylated tau epitopes Ser198 and Ser262. ■ 4 and 60 days after SE: increased neuropeptide Y immunoreactivity in the amygdala.
Leroy et al., 2003 [80]	Systemic lithium + methyl-scopolamine + pilocarpine; 6–12 h	<ul style="list-style-type: none"> ■ 1 h after SE onset: 14C-2DG injected; 582% increase in local cerebral metabolic rate; ■ 4 h after SE: if 2 min SE duration, moderate intensity in Fos expression; if 30–240 min SE duration, strong Fos expression; ■ 24 h after SE: HSP72 and acid fuchsin strong in the amygdala in groups with 90 min or longer SE. ■ Immediately after SE, 1 and 4 weeks after SE: no alterations in T1- and T2-weighted MRI (visual inspection) ■ 1, 2, 4, and 8 h after SE onset: increased levels of caspase 3 in the amygdala. Colocalized with both glia (higher quantity) and neurons; not with microglia. ■ 16, 24, and 48 h after SE: higher increase in caspase 3 (peak at 16 h) in the lateral, basal, and medial amygdala; not increased in the central amygdala; ■ 48 h: Fluorojade B and TUNEL positive neurons increase. ■ 24 h after SE: increased VEGF expression in the astroglia and neurons, particularly striking in neurons in the amygdala ■ 4 months after SE: increased number of KCNQ2-expressing neurons in the basolateral amygdala. ■ 10 days, 1, 2, 3, and 4 months after SE: medial amygdaloid nucleus evaluated; reduced Timm staining at 10 days, gradually recovering to normal levels, completely normal at 4 months; synaptophysin peak at 10 days, returning back to normal levels at 3 months; MAP2 increased expression that was maintained during all times evaluated. ■ 2, 4, 12, 24, 48 h: Fos staining increased between 2 and 12 h in anterior parts, and between 2 and 24 h in posterior parts of the medial amygdaloid nucleus; Fos B presented a progressive increase, with peak at 48 h, but starting at 2 h in posterodorsal, 4 h in anterodorsal
Lintunen et al., 2005 [81]	Systemic kainic acid; at least 5 h	<ul style="list-style-type: none"> ■ 1 and 3 d after SE onset: no difference in IL-6 or GP130 expression relative to control. ■ 6 and 12 h after SE onset: increased IL-6 expression; GP130 expression continues at normal levels. ■ 1 and 3 d after SE onset: no difference in IL-6 or GP130 expression relative to control. ■ 7 days after SE onset: no difference in IL-6 expression relative to control; GP130 hyperregulation. ■ 90 min after SE onset: blood–brain barrier leak in the medial (66%), but not in the basolateral, amygdaloid nucleus; increased cerebral blood volume (generalized); ■ 2 months after SE: reduced cell count in the medial amygdaloid nucleus ■ Histamine H1 receptor mRNA expression after SE: not altered at 3 and 6 h; reduced expression levels at 12 h, 1, 2, 3, and 7 days; back to normal levels at 4 weeks, 6 months, and 1 year. ■ Histamine H1 receptor binding after SE: not altered at 3, 6, and 12 h; reduced at 1, 2, 3, and 7 days; back to normal levels at 6 months and 1 year. ■ Histamine H3 receptor mRNA expression after SE: not altered at 3 and 6 h; variable at 12 h (depending on the isoform); reduced at 1, 2, and 3 days; isoforms return to normal levels between 7 days and 4 weeks and maintain in normal levels 6–12 months. ■ Histamine H3 receptor binding after SE: not altered at 3, 6, and 12 h; reduced at 1, 2, 3, 7 days, 4 weeks, 6 months, and 1 year. ■ Histamine levels (HPLC): increased at 6 h, 1, 3, 7 days. ■ Histamine-reactive fibers: increased at 6 h, 1, 2, 3 days, 4 weeks; back to normal levels 1 year after SE. ■ 13 weeks after SE: reduced protein phosphatase 2A activity; reduced expression of its regulatory B unit PR55; increased ratio of phosphorylated tau epitopes Ser198 and Ser262. ■ 4 and 60 days after SE: increased neuropeptide Y immunoreactivity in the amygdala.
Liu et al., 2016 [82]	Systemic kainic acid; at least 4 h	<ul style="list-style-type: none"> ■ 4 and 60 days after SE: increased neuropeptide Y immunoreactivity in the amygdala.
Lurton and Cavalheiro, 1997 [83]	Systemic methyl-scopolamine + pilocarpine; 5–24 h	<ul style="list-style-type: none"> ■ 1 h after SE onset: 14C-2DG injected; 582% increase in local cerebral metabolic rate; ■ 4 h after SE: if 2 min SE duration, moderate intensity in Fos expression; if 30–240 min SE duration, strong Fos expression; ■ 24 h after SE: HSP72 and acid fuchsin strong in the amygdala in groups with 90 min or longer SE. ■ Immediately after SE, 1 and 4 weeks after SE: no alterations in T1- and T2-weighted MRI (visual inspection) ■ 1, 2, 4, and 8 h after SE onset: increased levels of caspase 3 in the amygdala. Colocalized with both glia (higher quantity) and neurons; not with microglia. ■ 16, 24, and 48 h after SE: higher increase in caspase 3 (peak at 16 h) in the lateral, basal, and medial amygdala; not increased in the central amygdala; ■ 48 h: Fluorojade B and TUNEL positive neurons increase. ■ 24 h after SE: increased VEGF expression in the astroglia and neurons, particularly striking in neurons in the amygdala ■ 4 months after SE: increased number of KCNQ2-expressing neurons in the basolateral amygdala. ■ 10 days, 1, 2, 3, and 4 months after SE: medial amygdaloid nucleus evaluated; reduced Timm staining at 10 days, gradually recovering to normal levels, completely normal at 4 months; synaptophysin peak at 10 days, returning back to normal levels at 3 months; MAP2 increased expression that was maintained during all times evaluated. ■ 2, 4, 12, 24, 48 h: Fos staining increased between 2 and 12 h in anterior parts, and between 2 and 24 h in posterior parts of the medial amygdaloid nucleus; Fos B presented a progressive increase, with peak at 48 h, but starting at 2 h in posterodorsal, 4 h in anterodorsal
Motte et al., 1998 [84]	Systemic lithium + pilocarpine; up to 10 h	<ul style="list-style-type: none"> ■ 1 h after SE onset: 14C-2DG injected; 582% increase in local cerebral metabolic rate; ■ 4 h after SE: if 2 min SE duration, moderate intensity in Fos expression; if 30–240 min SE duration, strong Fos expression; ■ 24 h after SE: HSP72 and acid fuchsin strong in the amygdala in groups with 90 min or longer SE. ■ Immediately after SE, 1 and 4 weeks after SE: no alterations in T1- and T2-weighted MRI (visual inspection) ■ 1, 2, 4, and 8 h after SE onset: increased levels of caspase 3 in the amygdala. Colocalized with both glia (higher quantity) and neurons; not with microglia. ■ 16, 24, and 48 h after SE: higher increase in caspase 3 (peak at 16 h) in the lateral, basal, and medial amygdala; not increased in the central amygdala; ■ 48 h: Fluorojade B and TUNEL positive neurons increase. ■ 24 h after SE: increased VEGF expression in the astroglia and neurons, particularly striking in neurons in the amygdala ■ 4 months after SE: increased number of KCNQ2-expressing neurons in the basolateral amygdala. ■ 10 days, 1, 2, 3, and 4 months after SE: medial amygdaloid nucleus evaluated; reduced Timm staining at 10 days, gradually recovering to normal levels, completely normal at 4 months; synaptophysin peak at 10 days, returning back to normal levels at 3 months; MAP2 increased expression that was maintained during all times evaluated. ■ 2, 4, 12, 24, 48 h: Fos staining increased between 2 and 12 h in anterior parts, and between 2 and 24 h in posterior parts of the medial amygdaloid nucleus; Fos B presented a progressive increase, with peak at 48 h, but starting at 2 h in posterodorsal, 4 h in anterodorsal
Nakasu et al., 1993 [85]	Systemic kainic acid; at least 1 h	<ul style="list-style-type: none"> ■ 1 h after SE onset: 14C-2DG injected; 582% increase in local cerebral metabolic rate; ■ 4 h after SE: if 2 min SE duration, moderate intensity in Fos expression; if 30–240 min SE duration, strong Fos expression; ■ 24 h after SE: HSP72 and acid fuchsin strong in the amygdala in groups with 90 min or longer SE. ■ Immediately after SE, 1 and 4 weeks after SE: no alterations in T1- and T2-weighted MRI (visual inspection) ■ 1, 2, 4, and 8 h after SE onset: increased levels of caspase 3 in the amygdala. Colocalized with both glia (higher quantity) and neurons; not with microglia. ■ 16, 24, and 48 h after SE: higher increase in caspase 3 (peak at 16 h) in the lateral, basal, and medial amygdala; not increased in the central amygdala; ■ 48 h: Fluorojade B and TUNEL positive neurons increase. ■ 24 h after SE: increased VEGF expression in the astroglia and neurons, particularly striking in neurons in the amygdala ■ 4 months after SE: increased number of KCNQ2-expressing neurons in the basolateral amygdala. ■ 10 days, 1, 2, 3, and 4 months after SE: medial amygdaloid nucleus evaluated; reduced Timm staining at 10 days, gradually recovering to normal levels, completely normal at 4 months; synaptophysin peak at 10 days, returning back to normal levels at 3 months; MAP2 increased expression that was maintained during all times evaluated. ■ 2, 4, 12, 24, 48 h: Fos staining increased between 2 and 12 h in anterior parts, and between 2 and 24 h in posterior parts of the medial amygdaloid nucleus; Fos B presented a progressive increase, with peak at 48 h, but starting at 2 h in posterodorsal, 4 h in anterodorsal
Narkilahti et al., 2003 [86]	Systemic kainic acid; 6–12 h	<ul style="list-style-type: none"> ■ 1 h after SE onset: 14C-2DG injected; 582% increase in local cerebral metabolic rate; ■ 4 h after SE: if 2 min SE duration, moderate intensity in Fos expression; if 30–240 min SE duration, strong Fos expression; ■ 24 h after SE: HSP72 and acid fuchsin strong in the amygdala in groups with 90 min or longer SE. ■ Immediately after SE, 1 and 4 weeks after SE: no alterations in T1- and T2-weighted MRI (visual inspection) ■ 1, 2, 4, and 8 h after SE onset: increased levels of caspase 3 in the amygdala. Colocalized with both glia (higher quantity) and neurons; not with microglia. ■ 16, 24, and 48 h after SE: higher increase in caspase 3 (peak at 16 h) in the lateral, basal, and medial amygdala; not increased in the central amygdala; ■ 48 h: Fluorojade B and TUNEL positive neurons increase. ■ 24 h after SE: increased VEGF expression in the astroglia and neurons, particularly striking in neurons in the amygdala ■ 4 months after SE: increased number of KCNQ2-expressing neurons in the basolateral amygdala. ■ 10 days, 1, 2, 3, and 4 months after SE: medial amygdaloid nucleus evaluated; reduced Timm staining at 10 days, gradually recovering to normal levels, completely normal at 4 months; synaptophysin peak at 10 days, returning back to normal levels at 3 months; MAP2 increased expression that was maintained during all times evaluated. ■ 2, 4, 12, 24, 48 h: Fos staining increased between 2 and 12 h in anterior parts, and between 2 and 24 h in posterior parts of the medial amygdaloid nucleus; Fos B presented a progressive increase, with peak at 48 h, but starting at 2 h in posterodorsal, 4 h in anterodorsal
Nicoletti et al., 2008 [87]	Systemic atropine methylbromide + pilocarpine; 1 h	<ul style="list-style-type: none"> ■ 1 h after SE onset: 14C-2DG injected; 582% increase in local cerebral metabolic rate; ■ 4 h after SE: if 2 min SE duration, moderate intensity in Fos expression; if 30–240 min SE duration, strong Fos expression; ■ 24 h after SE: HSP72 and acid fuchsin strong in the amygdala in groups with 90 min or longer SE. ■ Immediately after SE, 1 and 4 weeks after SE: no alterations in T1- and T2-weighted MRI (visual inspection) ■ 1, 2, 4, and 8 h after SE onset: increased levels of caspase 3 in the amygdala. Colocalized with both glia (higher quantity) and neurons; not with microglia. ■ 16, 24, and 48 h after SE: higher increase in caspase 3 (peak at 16 h) in the lateral, basal, and medial amygdala; not increased in the central amygdala; ■ 48 h: Fluorojade B and TUNEL positive neurons increase. ■ 24 h after SE: increased VEGF expression in the astroglia and neurons, particularly striking in neurons in the amygdala ■ 4 months after SE: increased number of KCNQ2-expressing neurons in the basolateral amygdala. ■ 10 days, 1, 2, 3, and 4 months after SE: medial amygdaloid nucleus evaluated; reduced Timm staining at 10 days, gradually recovering to normal levels, completely normal at 4 months; synaptophysin peak at 10 days, returning back to normal levels at 3 months; MAP2 increased expression that was maintained during all times evaluated. ■ 2, 4, 12, 24, 48 h: Fos staining increased between 2 and 12 h in anterior parts, and between 2 and 24 h in posterior parts of the medial amygdaloid nucleus; Fos B presented a progressive increase, with peak at 48 h, but starting at 2 h in posterodorsal, 4 h in anterodorsal
Penschuck et al., 2005 [88]	Ventral hippocampus electrical stimulation; at least 2 h	<ul style="list-style-type: none"> ■ 1 h after SE onset: 14C-2DG injected; 582% increase in local cerebral metabolic rate; ■ 4 h after SE: if 2 min SE duration, moderate intensity in Fos expression; if 30–240 min SE duration, strong Fos expression; ■ 24 h after SE: HSP72 and acid fuchsin strong in the amygdala in groups with 90 min or longer SE. ■ Immediately after SE, 1 and 4 weeks after SE: no alterations in T1- and T2-weighted MRI (visual inspection) ■ 1, 2, 4, and 8 h after SE onset: increased levels of caspase 3 in the amygdala. Colocalized with both glia (higher quantity) and neurons; not with microglia. ■ 16, 24, and 48 h after SE: higher increase in caspase 3 (peak at 16 h) in the lateral, basal, and medial amygdala; not increased in the central amygdala; ■ 48 h: Fluorojade B and TUNEL positive neurons increase. ■ 24 h after SE: increased VEGF expression in the astroglia and neurons, particularly striking in neurons in the amygdala ■ 4 months after SE: increased number of KCNQ2-expressing neurons in the basolateral amygdala. ■ 10 days, 1, 2, 3, and 4 months after SE: medial amygdaloid nucleus evaluated; reduced Timm staining at 10 days, gradually recovering to normal levels, completely normal at 4 months; synaptophysin peak at 10 days, returning back to normal levels at 3 months; MAP2 increased expression that was maintained during all times evaluated. ■ 2, 4, 12, 24, 48 h: Fos staining increased between 2 and 12 h in anterior parts, and between 2 and 24 h in posterior parts of the medial amygdaloid nucleus; Fos B presented a progressive increase, with peak at 48 h, but starting at 2 h in posterodorsal, 4 h in anterodorsal
Pereno and Beltramino, 2010 [89]	Systemic kainic acid; at least 3 h	<ul style="list-style-type: none"> ■ 1 h after SE onset: 14C-2DG injected; 582% increase in local cerebral metabolic rate; ■ 4 h after SE: if 2 min SE duration, moderate intensity in Fos expression; if 30–240 min SE duration, strong Fos expression; ■ 24 h after SE: HSP72 and acid fuchsin strong in the amygdala in groups with 90 min or longer SE. ■ Immediately after SE, 1 and 4 weeks after SE: no alterations in T1- and T2-weighted MRI (visual inspection) ■ 1, 2, 4, and 8 h after SE onset: increased levels of caspase 3 in the amygdala. Colocalized with both glia (higher quantity) and neurons; not with microglia. ■ 16, 24, and 48 h after SE: higher increase in caspase 3 (peak at 16 h) in the lateral, basal, and medial amygdala; not increased in the central amygdala; ■ 48 h: Fluorojade B and TUNEL positive neurons increase. ■ 24 h after SE: increased VEGF expression in the astroglia and neurons, particularly striking in neurons in the amygdala ■ 4 months after SE: increased number of KCNQ2-expressing neurons in the basolateral amygdala. ■ 10 days, 1, 2, 3, and 4 months after SE: medial amygdaloid nucleus evaluated; reduced Timm staining at 10 days, gradually recovering to normal levels, completely normal at 4 months; synaptophysin peak at 10 days, returning back to normal levels at 3 months; MAP2 increased expression that was maintained during all times evaluated. ■ 2, 4, 12, 24, 48 h: Fos staining increased between 2 and 12 h in anterior parts, and between 2 and 24 h in posterior parts of the medial amygdaloid nucleus; Fos B presented a progressive increase, with peak at 48 h, but starting at 2 h in posterodorsal, 4 h in anterodorsal
Pereno, Balaszczuk and Beltramino, 2011 [90]	Systemic kainic acid; at least 3 h	<ul style="list-style-type: none"> ■ 1 h after SE onset: 14C-2DG injected; 582% increase in local cerebral metabolic rate; ■ 4 h after SE: if 2 min SE duration, moderate intensity in Fos expression; if 30–240 min SE duration, strong Fos expression; ■ 24 h after SE: HSP72 and acid fuchsin strong in the amygdala in groups with 90 min or longer SE. ■ Immediately after SE, 1 and 4 weeks after SE: no alterations in T1- and T2-weighted MRI (visual inspection) ■ 1, 2, 4, and 8 h after SE onset: increased levels of caspase 3 in the amygdala. Colocalized with both glia (higher quantity) and neurons; not with microglia. ■ 16, 24, and 48 h after SE: higher increase in caspase 3 (peak at 16 h) in the lateral, basal, and medial amygdala; not increased in the central amygdala; ■ 48 h: Fluorojade B and TUNEL positive neurons increase. ■ 24 h after SE: increased VEGF expression in the astroglia and neurons, particularly striking in neurons in the amygdala ■ 4 months after SE: increased number of KCNQ2-expressing neurons in the basolateral amygdala. ■ 10 days, 1, 2, 3, and 4 months after SE: medial amygdaloid nucleus evaluated; reduced Timm staining at 10 days, gradually recovering to normal levels, completely normal at 4 months; synaptophysin peak at 10 days, returning back to normal levels at 3 months; MAP2 increased expression that was maintained during all times evaluated. ■ 2, 4, 12, 24, 48 h: Fos staining increased between 2 and 12 h in anterior parts, and between 2 and 24 h in posterior parts of the medial amygdaloid nucleus; Fos B presented a progressive increase, with peak at 48 h, but starting at 2 h in posterodorsal, 4 h in anterodorsal

(continued on next page)

Table 1 (continued)

Authors	SE induction method; SE duration	Data
Perez-Cruz and Rocha, 2002 [91] Pirttila et al., 2001 [92]	Systemic kainic acid; at least 2 h Systemic kainic acid; SE duration not informed	and posteroventral, and 12 h in the anteroventral medial amygdaloid nucleus; silver impregnation was increased in all areas from 12 to 48 h, with peak at 24 h. ■ 1 and 40 days after SE: μ -opioid receptors binding increased in all amygdaloid areas evaluated (anterior, medial, basolateral, and central) ■ 2 h and 4 h after SE induction: no neuronal loss. ■ 8 h after SE induction: the lateral nucleus starts to present reduced cell count. ■ 10 days, 4–8 weeks after SE: neuronal count less than 50% of control in the lateral nucleus ■ 10 days: gliosis peak in the lateral nucleus. ■ Central nucleus preserved. ■ MRI correlated to damage: reduced T2-weighted signal indicates medium to severe tissue damage. ■ 14 days after SE: 25% reduction in number of somatostatin-positive neurons in the lateral and in the basal nuclei of the amygdala; some rats with high score silver impregnation in the lateral nucleus (4/9) and mild–moderate–severe (1 each) impregnation in the basal nucleus (total 3/9). ■ 4 h after SE: 13–16% reduced cytochrome c oxidase activity in the medial amygdala as compared with control. No alteration in lactate dehydrogenase. ■ 24 h after SE: cytochrome c oxidase activity in the medial amygdala, as compared with control, maintains reduced, not as much as previous time. No alteration in lactate dehydrogenase. ■ 2 weeks after SE: cytochrome c oxidase back to normal levels. No alterations in lactate dehydrogenase activity. ■ 3 h, 1, 2, 3, and 9 days: T2-weighted MRI increased from 1 to 3 days in the amygdala. 1 day after SE, reduced apparent diffusion coefficient. ■ 24 h, 2, and 9 weeks after SE: progressive cell loss detected in the amygdala. ■ T2-weighted MRI increased in 2 waves, one with peak at 24 h and other starting at about 3 weeks and persisting until 9 weeks. Data collected at 2, 6, 24, 30 h, 2, 3, 7, 14, 21 days, and 5, 7, 9 weeks ■ ^{14}C -2DG injected 2 h after kainic acid, in rats presenting self-sustained SE; tissue collected 45 min later; autoradiography showed increased local cerebral glucose uptake in the amygdala ipsilateral to injection site. ■ Increased local cerebral glucose uptake in the amygdala (about 30%) ■ 4 h: highly increased local cerebral glucose uptake in the medial, basolateral, lateral amygdala nuclei; cerebral blood flow increased in the same areas; ■ 24 h, 7 days: numerous Fluorjade B-positive neurons in the basolateral amygdala (other areas not evaluated) ■ 3 days after SE induction: IL-1b, IL-6, and TNF-alpha levels increased when compared with control; GAT-1 and GAT-3 expressions increased when compared with control. ■ 2 days after SE: increased T2 relaxation time (+17%); ■ 7 and 30 days after SE: T2 relaxation time not different from baseline; ■ 2, 7, and 30 days after SE: no amygdala volume alterations were observed. ■ 10 weeks after SE: severe neuronal loss basolateral amygdala.
Righini et al., 1994 [95] Roch et al., 2002 [96]	Systemic kainic acid; at least 1 h Systemic lithium + methyl scopolamine + pilocarpine; at least 2 h	
Sawamura et al., 2001 [97]	Local, unilateral kainic acid in <i>substantia nigra pars reticulata</i> ; at least 3 h	
Scorza et al., 2002 [98] Silva et al., 2011 [99]	Systemic pilocarpine; 6 h Systemic methyl-scopolamine + pilocarpine; at least 4 h	
Su et al., 2015 [100] Suleymanova, Gulyaev and Abbasova, 2016 [101] Tchekalarova et al., 2017 [102]	Local intracerebroventricular injection of kainic acid; 1–2 h Systemic lithium + pilocarpine; at least 2 h. Systemic kainic acid; at least 3 h	
Turski et al., 1983 [17] Tuunanen et al., 1999 [103]	Systemic methyl-scopolamine + pilocarpine; 5–6 h Systemic kainic acid; at least 7 h	
Tuunanen, Halonen and Pitkanen, 1996 [104]	Systemic kainic acid or perforant path electrical stimulation; 10–16 h and 35–55 min, respectively	■ 1 day after SE: extensive damage to the amygdala. ■ Extensive study; amygdala divided in the deep nuclei (lateral, basal, accessory basal), superficial nuclei (medial, anterior cortical, posterior cortical, periamygdaloid cortex, nucleus of the lateral olfactory tract, and bed nucleus of the accessory olfactory tract), and remaining nuclei (anterior amygdaloid area, intercalated nucleus, central nucleus, and the amygdalohippocampal area). ■ TUNEL increased progressively in most areas, with the exception of the anterior amygdaloid area (not stained) and the central nucleus (peaks at 16 and 48 h) ■ Silver staining: progressive increase, with stabilization at 4 h in the central nucleus, medial nucleus, basal nucleus; and stabilization at 16 h in the anterior amygdaloid area. ■ Thionin staining showed progressive cell loss in most nuclei. ■ Dorsal part of the lateral, basal, central, and medial nuclei, anterior amygdaloid area, and bed nucleus of the accessory olfactory tract were less affected than others (as per silver and thionin evaluations) ■ Bax and Bcl2 were evaluated in the lateral and basal nuclei, with no alterations in both, except for a peak in Bax-ir neurons in the lateral nucleus at 2 h after SE and a loss of such neurons from 24 to 48 h. ■ 2 days and 2 weeks after SE (kainic acid only, all animals presented damage), damage score based on silver impregnation, somatostatin, and GABA stainings: detailed evaluation; some data are as follows: virtually all nuclei from the amygdala had some degree of damage; noticeable lateral nucleus (ventrolateral and medial), basal nucleus (parvicellular division), accessory basal nucleus, ventral portion of the central division of the medial nucleus, periamygdaloid cortex, amygdalohippocampal area, and posterior cortical nucleus. ■ 2 weeks after SE (kainic acid), density of GABA-positive neurons: reduced to 56% in the lateral nucleus and to 25% in the basal nucleus; somatostatin-positive neurons: reduced to 48% in the lateral nucleus and to 33% in the basal nucleus. Specially, great loss of somatostatin-positive neurons was seen in areas apparently preserved by silver staining and Nissl, such as intermediate and magnocellular divisions of the basal nucleus. ■ 2 weeks after SE (perforant path; 4 out of 9 presented damage) was mostly preserved, with some degree of damage in the medial division of the lateral nucleus and ventral portion of the central division of the medial nucleus. Somatostatin-positive neurons were reduced to 76% in the lateral nucleus and to 75% in the basal nucleus. ■ 3 and 5 h after SE onset: decreased T2-weighted MRI signal and apparent diffusion
van Eijnsden et al., 2004	Systemic lithium + methyl scopolamine +	

Table 1 (continued)

Authors	SE induction method; SE duration	Data
[105] van Vliet et al., 2014 [106]	pilocarpine; 7 h (under anesthesia) Systemic kainic acid; at least 4 h	coefficient at both times. ■ 1 and 6 weeks after SE: blood–brain barrier leakage in the amygdala, peak at 24 h; Control is the same animal before SE. ■ 6 weeks after SE, neuronal loss confirmed by Nissl staining and blood–brain barrier leakage confirmed by fluorescein detection. ■ 1, 4, 8 days, 3 and 6 weeks after SE: blood–brain barrier leakage (MRI) in the amygdala in all time points. Control is the same rat before SE. ■ 30 and 120 min: no alterations ■ 1, 7, 14 days: number of neurons reduced progressively; caspase 3 marked predominantly in neurons, at 1 and 7 days (peak), and back to normal levels at day 14; TUNEL presented the same pattern as caspase 3. ■ 47 days after SE induction: reduced neuronal survival (Neu-N positive cells counted), maintenance of parvalbumin-positive neurons, increased optical density parvalbumin reading.
van Vliet et al., 2016 [107]	Systemic kainic acid; at least 2 h.	
Weise et al., 2005 [108]	Systemic methyl scopolamine + pilocarpine; 6–8 h	
Wolf et al., 2016 [109]	Systemic lithium + methyl-scopolamine + pilocarpine; at least 2 h	
Yamada et al., 2009 [110]	Systemic lithium + methyl-scopolamine + pilocarpine; 91–136 min	
Yang et al., 2016 [111]	Local, intracerebroventricular kainic acid injection; “at least 1–2 h”	

Abbreviations: DOPAC: 3,4-dihydroxyphenylacetic acid; HVA: homovanillic acid; HPLC: high-performance liquid chromatography; KA: kainic acid; ATP: Adenosine-5'-triphosphate; ADP: adenosine diphosphate; AMP: adenosine monophosphate; TUNEL: terminal deoxynucleotidyl transferase dUTP nick end labeling (dUTP = deoxyuridine 5'-triphosphate).

higher receptor recycling process [100]. The synaptic reorganization in the amygdala neuronal terminals is also evidenced 7–10 days after SE. In this time range, glutamatergic receptors such as kainate type 1 (GLUK1) are reduced [68], while levels of GAD65/67 isoforms [68], and of cytokine receptor GP130 [79], are increased.

The progressive loss of amygdala neurons and of amygdala volume, as mentioned before, starts hours after SE and reaches maximal intensity months later, with profound modifications been reported [54,58,77,78,80,89,90,92,96,102,104,108,59,109,62–64,67,71,75,76]. Among the lost neurons, there is a preferential reduction of GABAergic neurons immunoreactive to somatostatin, but GABAergic neurons in general are lost in the same proportion as the total population [66,68,93,104]. Still in the long-term, blood–brain barrier integrity is compromised in the amygdala [106,107]. Additionally, blood vessel density is increased [73], and eventual alterations in T2-weighted signal are observed [96]. Four to six months after SE, the amygdala presents increased number of neurons expressing the member 2 of the subfamily Q (KCNQ2) voltage-gated potassium channels [88]. In addition, protein phosphatase 2A activity and its regulatory B unit PR55 are reduced, with concomitant increase in phosphorylated tau epitopes [82]. Furthermore, angiotensin II receptor type 1 is reduced [51]. Gliosis is still observed [124], but microglia marked by OX42 [75] and histamine receptor H1 [81] return to normal levels. Lastly, the H3 receptors stay reduced up to one year after SE [81].

4. Discussion and concluding remarks

Epilepsy and epileptogenesis are emergent properties of complex systems made of multifactorial phenomena [7,125,126]. They can involve different brain areas and occur because of genetic and developmental factors, or they can develop after diverse brain insults, stimulations, injuries, and infections [127–129]. A great number of animal models have been developed, allowing for the better understanding of epilepsy, the discovery of new and better treatments, and the elucidation of morphological and molecular mechanisms underlying seizures and epileptogenesis [13,130–135]. Despite the above statements, a significant parcel of the patients with temporal lobe epilepsy remains pharmacoresistant [136–138].

In the current study, we aimed to organize the data on the participation of the amygdaloid complex as a whole and its nuclei in epileptogenesis, considering histopathological, morphological, and imaging techniques. We were able to classify several alterations in the

amygdala during and after SE: energy metabolism, neuroprotection, circulatory and fluid regulation, neurotransmission, immediate early genes, tissue damage, inflammation, plasticity, and cell suffering. It is important to note that any conclusions are hindered by the lack of details in most results descriptions (amygdaloid complex's several nuclei become simply “amygdala” or “amygdaloid complex”), great variability in protocols for SE induction and duration, and animal's age and strain. Besides, there is concentration of results in some time points after SE. For example, there is a great amount of data 2 h and 24 h after SE, while much less is known about the other time points. Additionally, nonexpected alterations were scarcely investigated. For example, if Pereno and collaborators [90] did not immunostain Fos and Fos B in materials that were not produced specifically to the optimal time range of those molecules' expression (Fos peaks at 2–4 h after SE and Fos B peaks at 48 h after SE), it would not be possible to know that both can be observed 24 h after SE in the medial amygdaloid nucleus. Thus, in general, there is little negative data and even less unexpected data been generated in epilepsy research.

As can be seen in Fig. 2 of the current review, several alterations are observed in the amygdaloid complex during and after SE induction in young adult and adult rats. For example, among all the categories classified in our review, there is strong evidence for plastic changes that lead to altered circuitry and functionality in the amygdala. The neurotransmission systems involved with the activation, propagation, and/or maintenance of epileptic seizures are complex and relate to regulatory processes of excitation and inhibition in several brain areas [139]. SE physiopathology involves a failure in the mechanisms that normally prevent the occurrence of an isolated epileptic seizure; caused by excessive excitation and/or inefficient inhibition [140–142]. The plastic manifestations in the adult CNS are characterized by dendritic alterations, synaptic restructuring, axonal outgrowth, dendritic reorganization, synaptogenesis, and neurogenesis [143–146], all those observed in the amygdala. It is suggested that spontaneous recurrent seizures in temporal lobe epilepsy models result from this excessive, dysfunctional plasticity, leading to pathological expressions of the neuronal function [22,147,148]. The great plastic ability of neural tissue given by SE-induced gene expression, concurrent with cell loss and therefore, clearance of local connective sites, is accepted as part of the mechanisms underlying epileptogenesis in SE models of temporal lobe epilepsy [149]. All the data categorized in the current review, referring to the amygdaloid complex, indicate that this structure is deeply involved in the pathophysiology of epilepsy.

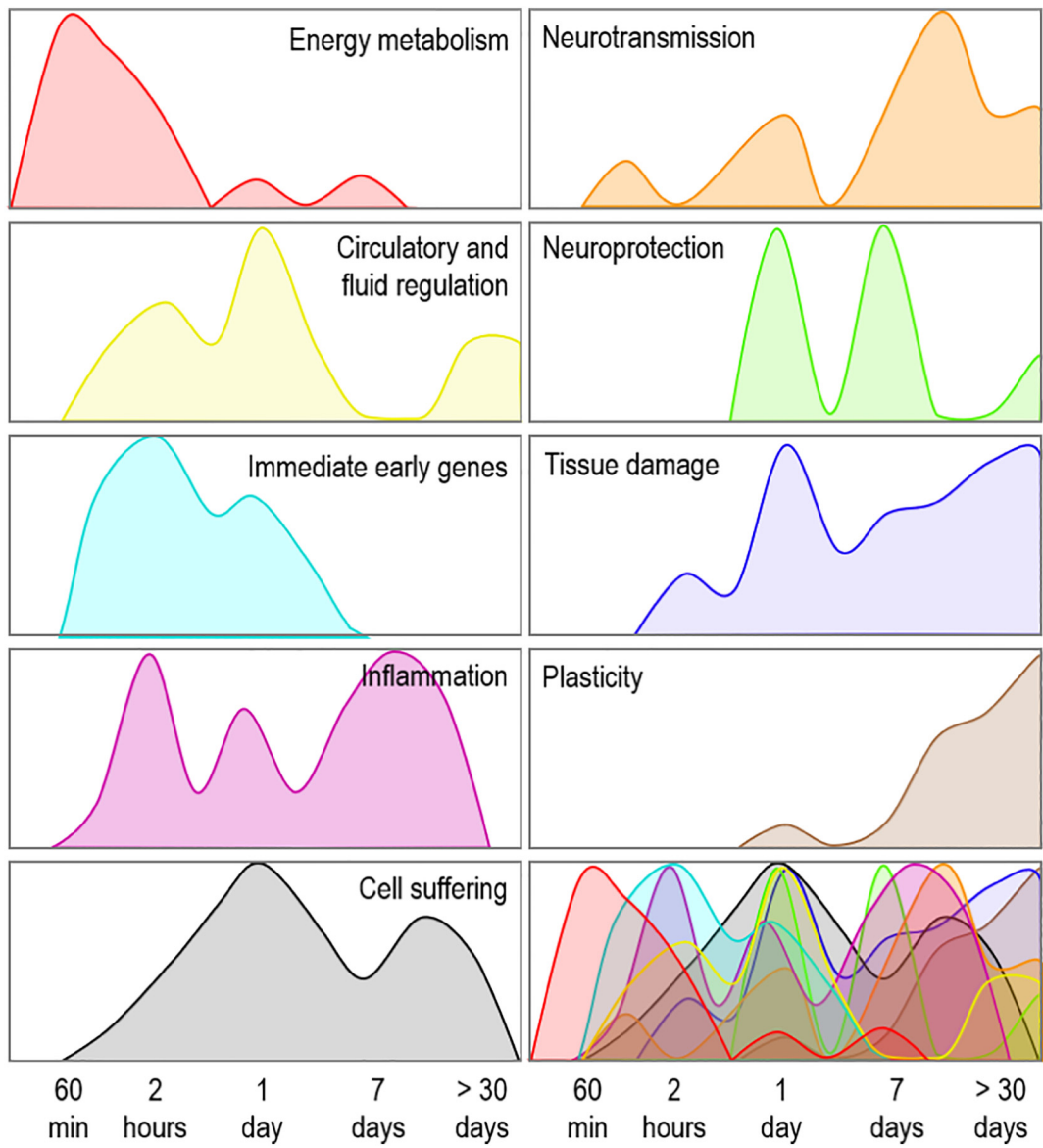


Fig. 2. Timeline of anatomopathological alterations observed in the amygdala after status epilepticus. Note that the time axis is nonlinear, since the amount of data in each time point is variable. This figure illustrates a qualitative evaluation of the evidence found for each pathological process category listed below. Higher curves indicate greater evidence, based on the intensity of the described alterations, in the underlying time point. Pathological process categories: Energy metabolism, Circulatory and fluid regulation, Immediate early genes expression, Inflammation, Cell suffering, Neuroprotection, Neurotransmission, Tissue damage, and Plasticity. Y-axis: arbitrary scale.

It is important to note, however, that the translation of research findings in animal models to the human context is complex. For instance, current animal models of epilepsy do not reflect the diverse etiologic nature of epilepsy, nor are the new drugs discovered using animal models more effective in avoiding pharmacoresistance [150–152]. Moreover, a parallel between human and rodent amygdaloid nuclei may be hampered by its several morphofunctional differences or poor data availability [40,153,154]. Comparison between both species have revealed differences in amygdaloid complex nuclei volumes, neuronal sizes, neuronal density, neuropil volume, interneuron composition and distribution, and monoamine transporters [154–156], implying greater functional complexity in human amygdala than in rats. Nonetheless, many other evidences support similarities between human and rat functional and epilepsy-related anatomopathological characteristics [12,40]. For instance, human and rodents' amygdala have the same function of identifying threatening situations, emotional learning, and fear conditioning [157–160]. Specifically, amygdala atrophy in human patients with epilepsy have been consistently shown, such as in animal models [36,40,41,161]. In fact, amygdala volume was inversely

correlated to the number of epileptic seizures in chronic temporal lobe epilepsy in humans [162].

Nonetheless, there is a much greater number of studies considering hippocampal alterations after SE [163,164], when compared with those in the amygdala. The reasons why this happens are not clear, but one possible explanation is the neatly organized and well-known hippocampal anatomy, as opposed to the amygdala complex and less conspicuous anatomical and functional organization [165–170]. Despite the above, amygdaloid complex's contribution to epileptogenic process is demonstrated by the accumulating evidence reviewed here and elsewhere [40–43]. In general, the process starts with metabolic alterations, followed by inflammatory process development. Neurotransmission and genetic expression are changed, together with plastic and proliferative phenomena. Finally, cell death leads to the long-term atrophy and loss of functionality. This consequently results in seizures and in disturbances of mood, of emotional memories, and of cognition. Considering that the amygdala is extensively connected to several other brain areas besides hippocampus, it is critical that research be reexamined in order to include other substrates in the exploration of the circuits

that take part in epilepsy and epileptogenesis. Thus, we suggest that attention should be directed to other areas besides hippocampus, in the characterization of pathophysiology of epilepsy.

It is interesting to highlight, additionally, that the amygdaloid complex is distributed in rat brains mostly in the same anteroposterior range as hippocampal formation [171]. Actually, in the exact same areas included in histopathological slices obtained for hippocampus evaluation, not only the amygdala can be observed, but also several cortices of interest for epilepsy (entorhinal, piriform, cingulate) and many other areas that may be of interest for epilepsy pathophysiology (the entire thalamus and hypothalamus, *substantia nigra*, periaqueductal gray matter, superior colliculus, mesencephalic tegmentum). Thus, it is probable that research laboratories that focus on hippocampal alterations consequent to SE may have, in their archives, histopathological material that can be used to investigate alterations in several other brain areas. Since it was not the purpose of this review, we did not compare results from the amygdala with those from hippocampus. However, a rapid inspection in the articles included in this review indicates that pathophysiology of epilepsy develops differently in both structures. Such differences have been described on intensity [66,83,99], time of presentation after the onset of SE [56], presence or absence of the studied variables [53,70,95], and even opposite findings between both structures [51,65]. In times when ethics in animal use for research raise concerns and the 3R strategies gain more attention [172–174], going back to high quality material stored in research laboratories could generate original shared research data on epilepsy and epileptogenesis, giving rise to new hypotheses for future investigations. This kind of approach and effort will be fundamental for actual multinational and multicenter research in Global Cooperation in epileptology.

Supplementary data to this article can be found online at <https://doi.org/10.1016/j.yebeh.2019.106831>.

Funding

This study was financed in part by: Coordenação de Aperfeiçoamento de Pessoal de Nível Superior - Brasil (CAPES) - Finance Code 001; FAPESP 2019/05957-8 and FAPESP 2014/50891-1 (INCT); Conselho Nacional de Desenvolvimento Científico e Tecnológico (CNPQ) 428188/2016-8, 309397/2018-9 and 408707/2018-6; National Institute of Science and Technology (INCT) – MCTI/CNPq/CAPES/FAPs nº 16/2014; Fundação de Amparo à Pesquisa do Estado de Minas Gerais (FAPEMIG) APQ 02485-15; Fundação de Amparo à Pesquisa do Estado de Alagoas (FAPEAL). NGC holds a CNPq-Brazil Research Fellowship.

References

- [1] Hirose S, Okada M, Kaneko S, Mitsudome A. Are some idiopathic epilepsies disorders of ion channels?: a working hypothesis. *Epilepsia* 2000;41:191–204.
- [2] Berkovic SF, Scheffer IE. Genetics of the epilepsies. *Epilepsia* 2001;42(Suppl. 5): 16–23.
- [3] Beghi E. Addressing the burden of epilepsy: many unmet needs. *Pharmacol Res* 2016;107:79–84. <https://doi.org/10.1016/j.phrs.2016.03.003>.
- [4] WHO. *Epilepsy: a public health imperative* Geneva ; 2019 [doi:978-92-4-151593-1].
- [5] Fisher RS, van Emde Boas W, Blume W, Elger C, Genton P, Lee P, et al. Epileptic seizures and epilepsy: definitions proposed by the International League Against Epilepsy (ILAE) and the International Bureau for Epilepsy (IBE). *Epilepsia* 2005;46: 470–2. <https://doi.org/10.1111/j.0013-9580.2005.66104.x>.
- [6] Thurman DJ, Beghi E, Begley CE, Berg AT, Buchhalter JR, Ding D, et al. Standards for epidemiologic studies and surveillance of epilepsy. *Epilepsia* 2011;52(Suppl. 7): 2–26. <https://doi.org/10.1111/j.1528-1167.2011.03121.x>.
- [7] Sloviter RS. Epileptogenesis meets Occam's Razor. *Curr Opin Pharmacol* 2017;35: 105–10. <https://doi.org/10.1016/j.coph.2017.07.012>.
- [8] Pinel JP, Rovner LL. Experimental epileptogenesis: kindling-induced epilepsy in rats. *Exp Neurol* 1978;58:190–202.
- [9] Turski L, Ikonomidou C, Turski WA, Bortolotto ZA, Cavalheiro EA. Review: cholinergic mechanisms and epileptogenesis. The seizures induced by pilocarpine: a novel experimental model of intractable epilepsy. *Synapse* 1989;3:154–71. <https://doi.org/10.1002/syn.890030207>.
- [10] Pitkänen A, Lukasiuk K, Dudek FE, Staley KJ. Epileptogenesis. *Cold Spring Harb Perspect Med* 2015;5. <https://doi.org/10.1101/cshperspect.a022822>.
- [11] Loscher W, Brandt C. High seizure frequency prior to antiepileptic treatment is a predictor of pharmacoresistant epilepsy in a rat model of temporal lobe epilepsy. *Epilepsia* 2010;51:89–97. <https://doi.org/10.1111/j.1528-1167.2009.02183.x>.
- [12] Kandratavicius L, Balista PA, Lopes-Aguiar C, Ruggiero RN, Umeoka EH, Garcia-Cairasco N, et al. Animal models of epilepsy: use and limitations. *Neuropsychiatr Dis Treat* 2014;10:1693–705. <https://doi.org/10.2147/NDT.S50371>.
- [13] Gorter JA, van Vliet EA, Lopes da Silva FH. Which insights have we gained from the kindling and post-status epilepticus models? *J Neurosci Methods* 2016;260: 96–108. <https://doi.org/10.1016/j.jneumeth.2015.03.025>.
- [14] Leite JP, Garcia-Cairasco N, Cavalheiro EA. New insights from the use of pilocarpine and kainate models. *Epilepsia Res* 2002;50:93–103.
- [15] Goddard GV. Development of epileptic seizures through brain stimulation at low intensity. *Nature* 1967;214:1020–1.
- [16] Goddard GV, McIntyre DC, Leech CK. A permanent change in brain function resulting from daily electrical stimulation. *Exp Neurol* 1969;25:295–330.
- [17] Turski WA, Cavalheiro EA, Schwarz M, Czuczwar SJ, Kleinrok Z, Turski L. Limbic seizures produced by pilocarpine in rats: behavioral, electroencephalographic and neuropathological study. *Behav Brain Res* 1983;9:315–35.
- [18] Lothman EW, Bertram 3rd EH. Epileptogenic effects of *status epilepticus*. *Epilepsia* 1993;34(Suppl. 1):S59–70.
- [19] Trinka E, Kälväinen R. 25 years of advances in the definition, classification and treatment of *status epilepticus*. *Seizure* 2017;44:65–73. <https://doi.org/10.1016/j.seizure.2016.11.001>.
- [20] Navidhamidi M, Ghasemi M, Mehranfar N. Epilepsy-associated alterations in hippocampal excitability. *Rev Neurosci* 2017;28:307–34. <https://doi.org/10.1515/reneuro-2016-0059>.
- [21] Thom M. Review: hippocampal sclerosis in epilepsy: a neuropathology review. *Neuropathol Appl Neurobiol* 2014;40:520–43. <https://doi.org/10.1111/nan.12150>.
- [22] Bonansco C, Fuenzalida M. Plasticity of hippocampal excitatory-inhibitory balance: missing the synaptic control in the epileptic brain. *Neural Plast* 2016; 2016:8607038. <https://doi.org/10.1155/2016/8607038>.
- [23] Kairiss EW, Racine RJ, Smith GK. The development of the interictal spike during kindling in the rat. *Brain Res* 1984;322:101–10.
- [24] Racine RJ, Paxinos G, Mosher JM, Kairiss EW. The effects of various lesions and knife-cuts on septal and amygdala kindling in the rat. *Brain Res* 1988;454:264–74.
- [25] Handforth A, Ackermann RF. Electrogenetic *status epilepticus* induced from numerous limbic sites. *Epilepsia Res* 1993;15:21–6.
- [26] Mohapel P, Dufresne C, Kelly ME, McIntyre DC. Differential sensitivity of various temporal lobe structures in the rat to kindling and *status epilepticus* induction. *Epilepsia Res* 1996;23:179–87.
- [27] Apland JP, Aroniadou-Anderjaska V, Braga MFM. Soman induces ictogenesis in the amygdala and interictal activity in the hippocampus that are blocked by a GluR5 kainate receptor antagonist in vitro. *Neuroscience* 2009;159:380–9. <https://doi.org/10.1016/j.neuroscience.2008.11.053>.
- [28] Handforth A, Treiman DM. Functional mapping of the late stages of *status epilepticus* in the lithium-pilocarpine model in rat: a ¹⁴C-2-deoxyglucose study. *Neuroscience* 1995;64:1075–89.
- [29] Handforth A, Ackermann RF. Mapping of limbic seizure progressions utilizing the electrogenetic *status epilepticus* model and the ¹⁴C-2-deoxyglucose method. *Brain Res Brain Res Rev* 1995;20:1–23.
- [30] McIntyre DC, Racine RJ. Kindling mechanisms: current progress on an experimental epilepsy model. *Prog Neurobiol* 1986;27:1–12.
- [31] Patterson KP, Brennan GP, Curran M, Kinney-Lang E, Dube C, Rashid F, et al. Rapid, coordinate inflammatory responses after experimental febrile *status epilepticus*: implications for epileptogenesis. *ENeuro* 2015;2. <https://doi.org/10.1523/ENEURO.0034-15.2015>.
- [32] Bankstahl JP, Brandt C, Loscher W. Prolonged depth electrode implantation in the limbic system increases the severity of *status epilepticus* in rats. *Epilepsia Res* 2014;108:802–5. <https://doi.org/10.1016/j.epilepsires.2014.01.025>.
- [33] Kullmann DM. What's wrong with the amygdala in temporal lobe epilepsy? *Brain* 2011;134:2800–1. <https://doi.org/10.1093/brain/awr246>.
- [34] Graebenitz S, Kedo O, Speckmann E-J, Gorji A, Panneck H, Hans V, et al. Interictal-like network activity and receptor expression in the epileptic human lateral amygdala. *Brain* 2011;134:2929–47. <https://doi.org/10.1093/brain/awr202>.
- [35] Schramm J. Temporal lobe epilepsy surgery and the quest for optimal extent of resection: a review. *Epilepsia* 2008;49:1296–307. <https://doi.org/10.1111/j.1528-1167.2008.01604.x>.
- [36] Feindel W, Rasmussen T. Temporal lobectomy with amygdalectomy and minimal hippocampal resection: review of 100 cases. *Can J Neurol Sci* 1991;18:603–5.
- [37] Sah P, Faber ESL, Lopez De Armentia M, Power J. The amygdaloid complex: anatomy and physiology. *Physiol Rev* 2003;83:803–34. <https://doi.org/10.1152/physrev.00002.2003>.
- [38] Pitkänen A, Pikkarainen M, Nurminen N, Ylinen A. Reciprocal connections between the amygdala and the hippocampal formation, perirhinal cortex, and postrhinal cortex in rat. A review. *Ann N Y Acad Sci* 2000;911:369–91.
- [39] Harden CL. Sexuality in men and women with epilepsy. *CNS Spectr* 2006;11:13–8.
- [40] Aroniadou-Anderjaska V, Fritsch B, Qashu F, Braga MFM. Pathology and pathophysiology of the amygdala in epileptogenesis and epilepsy. *Epilepsia Res* 2008;78: 102–16. <https://doi.org/10.1016/j.epilepsires.2007.11.011>.

[41] Cota VR, Drabowski BMB, de Oliveira JC, Moraes MFD. The epileptic amygdala: toward the development of a neural prosthesis by temporally coded electrical stimulation. *J Neurosci Res* 2016;94:463–85. <https://doi.org/10.1002/jnr.23741>.

[42] Mears D, Pollard HB. Network science and the human brain: using graph theory to understand the brain and one of its hubs, the amygdala, in health and disease. *J Neurosci Res* 2016;94:590–605. <https://doi.org/10.1002/jnr.23705>.

[43] Yilmazer-Hanek D, O'Loughlin E, Mcdermott K. Contribution of amygdala pathology to comorbid emotional disturbances in temporal lobe epilepsy. *J Neurosci Res* 2016;94:486–503. <https://doi.org/10.1002/jnr.23689>.

[44] Woolley CS, Schwartzkroin PA. Hormonal effects on the brain. *Epilepsia* 1998;39 (Suppl. 8):S2–8.

[45] Scharfman HE, MacLusky NJ. Sex differences in the neurobiology of epilepsy: a pre-clinical perspective. *Neurobiol Dis* 2014;72(Pt B):180–92. <https://doi.org/10.1016/j.nbd.2014.07.004>.

[46] Mlsna LM, Koh S. Maturation-dependent behavioral deficits and cell injury in developing animals during the subacute postictal period. *Epilepsy Behav* 2013;29: 190–7. <https://doi.org/10.1016/j.yebeh.2013.07.018>.

[47] Nairismagi J, Pitkanen A, Kettunen MI, Kauppinen RA, Kubova H. Status epilepticus in 12-day-old rats leads to temporal lobe neurodegeneration and volume reduction: a histologic and MRI study. *Epilepsia* 2006;47:479–88. <https://doi.org/10.1111/j.1528-1167.2006.00455.x>.

[48] Cavalheiro EA, Silva DF, Turski WA, Calderazzo-Filho LS, Bortolotto ZA, Turski L. The susceptibility of rats to pilocarpine-induced seizures is age-dependent. *Brain Res* 1987;465:43–58.

[49] Beyenburg S, Stoffel-Wagner B, Bauer J, Watzka M, Blumcke I, Bidlingmaier F, et al. Neuroactive steroids and seizure susceptibility. *Epilepsy Res* 2001;44:141–53.

[50] Alam AM, Starr MS. Regional changes in brain dopamine utilization during status epilepticus in the rat induced by systemic pilocarpine and intrahippocampal carbachol. *Neuropharmacology* 1996;35:159–67.

[51] Atanassova D, Tchekalarova J, Ivanova N, Nenchovska Z, Pavlova E, Atanassova N, et al. Losartan suppresses the kainate-induced changes of angiotensin AT1 receptor expression in a model of comorbid hypertension and epilepsy. *Life Sci* 2018;193: 40–6. <https://doi.org/10.1016/j.lfs.2017.12.006>.

[52] Barone P, Morelli M, Ciccarelli G, Cozzolino A, Dejoanna G, Campanella G, et al. Expression of c-fos protein in the experimental epilepsy induced by pilocarpine. *Synapse* 1993;14:1–9. <https://doi.org/10.1002/syn.890140102>.

[53] Cavarsan CF, Tescarollo F, Tesone-Coelho C, Moraes RLT, Motta FLT, Blanco MM, et al. Pilocarpine-induced status epilepticus increases Homer1a and changes mGluR5 expression. *Epilepsy Res* 2012;101:253–60. <https://doi.org/10.1016/j.epilepsyres.2012.04.011>.

[54] Chen S, Buckmaster PS. Stereological analysis of forebrain regions in kainate-treated epileptic rats. *Brain Res* 2005;1057:141–52. <https://doi.org/10.1016/j.brainres.2005.07.058>.

[55] Choi H, Kim YK, Oh SW, Im H-J, Hwang DW, Kang H, et al. In vivo imaging of mGluR5 changes during epileptogenesis using [11C]ABP688 PET in pilocarpine-induced epilepsy rat model. *PLoS One* 2014;9:e92765. <https://doi.org/10.1371/journal.pone.0092765>.

[56] Covolan L, Mello LE. Temporal profile of neuronal injury following pilocarpine or kainic acid-induced status epilepticus. *Epilepsy Res* 2000;39:133–52.

[57] Dedeurwaerdere S, Callaghan PD, Pham T, Rahardjo GL, Amhaoul H, Berghofer P, et al. PET imaging of brain inflammation during early epileptogenesis in a rat model of temporal lobe epilepsy. *EJNMMI Res* 2012;2:60. <https://doi.org/10.1186/2191-219X-2-60>.

[58] Dos Santos JG, Longo BM, Blanco MM, Menezes de Oliveira MG, Mello LE. Behavioral changes resulting from the administration of cycloheximide in the pilocarpine model of epilepsy. *Brain Res* 2005;1066:37–48. <https://doi.org/10.1016/j.brainres.2005.09.037>.

[59] Dragunow M, Young D, Hughes P, MacGibbon G, Lawlor P, Singleton K, et al. Is c-Jun involved in nerve cell death following status epilepticus and hypoxic-ischaemic brain injury? *Brain Res Mol Brain Res* 1993;18:347–52.

[60] Dube C, Andre V, Covolan L, Ferrandon A, Marescaux C, Nehlig A, C-Fos, Jun D and HSP72 immunoreactivity, and neuronal injury following lithium-pilocarpine induced status epilepticus in immature and adult rats. *Brain Res Mol Brain Res* 1998;63:139–54.

[61] Ebisu T, Rooney WD, Graham SH, Weiner MW, Maudsley AA. N-acetylaspartate as an in vivo marker of neuronal viability in kainate-induced status epilepticus: 1H magnetic resonance spectroscopic imaging. *J Cereb Blood Flow Metab* 1994;14: 373–82. <https://doi.org/10.1038/jcbfm.1994.48>.

[62] Engelhorn T, Doerfler A, Weise J, Baehr M, Forsting M, Hufnagel A. Cerebral perfusion alterations during the acute phase of experimental generalized status epilepticus: prediction of survival by using perfusion-weighted MR imaging and histopathology. *AJNR Am J Neuroradiol* 2005;26:1563–70.

[63] Engelhorn T, Hufnagel A, Weise J, Baehr M, Doerfler A. Monitoring of acute generalized status epilepticus using multilocal diffusion MR imaging: early prediction of regional neuronal damage. *AJNR Am J Neuroradiol* 2007;28:321–7.

[64] Engelhorn T, Weise J, Hammes T, Bluemcke I, Hufnagel A, Doerfler A. Early diffusion-weighted MRI predicts regional neuronal damage in generalized status epilepticus in rats treated with diazepam. *Neurosci Lett* 2007;417:275–80. <https://doi.org/10.1016/j.neulet.2007.02.072>.

[65] Fabre PF, Marzola P, Sbarbati A, Bentivoglio M. Magnetic resonance imaging of changes elicited by status epilepticus in the rat brain: diffusion-weighted and T2-weighted images, regional blood volume maps, and direct correlation with tissue and cell damage. *Neuroimage* 2003;18:375–89.

[66] Figueiredo TH, Qashu F, Apland JP, Aroniadou-Anderjaska V, Souza AP, Braga MFM. The GluK1 (GluR5) kainate/(alpha)-amino-3-hydroxy-5-methyl-4-isoxazolepropionic acid receptor antagonist LY293558 reduces soman-induced seizures and neuropathology. *J Pharmacol Exp Ther* 2011;336:303–12. <https://doi.org/10.1124/jpet.110.171835>.

[67] Francois J, Germe K, Ferrandon A, Koning E, Nehlig A. Carisbamate has powerful disease-modifying effects in the lithium-pilocarpine model of temporal lobe epilepsy. *Neuropharmacology* 2011;61:313–28. <https://doi.org/10.1016/j.neuropharm.2011.04.018>.

[68] Fritsch B, Qashu F, Figueiredo TH, Aroniadou-Anderjaska V, Rogawski MA, Braga MFM. Pathological alterations in GABAergic interneurons and reduced tonic inhibition in the basolateral amygdala during epileptogenesis. *Neuroscience* 2009;163: 415–29. <https://doi.org/10.1016/j.neuroscience.2009.06.034>.

[69] Gupta RC, Dettbarn W-D. Prevention of kainic acid seizures-induced changes in levels of nitric oxide and high-energy phosphates by 7-nitroindazole in rat brain regions. *Brain Res* 2003;981:184–92.

[70] Gupta RC, Milatovic D, Zivin M, W-DD Dettbarn. Seizure-induced changes in energy metabolites and effects of N-tert-butyl-alpha-phenylnitroline (PNB) and vitamin E in rats. *Plugers Arch* 2000;440:R160–2. <https://doi.org/10.1007/s004240000047>.

[71] Halonen T, Nissinen J, Pitkanen A. Neuroprotective effect of remacemide hydrochloride in a perforant pathway stimulation model of status epilepticus in the rat. *Epilepsy Res* 1999;34:251–69.

[72] Hanaya R, Boehm N, Nehlig A. Dissociation of the immunoreactivity of synaptophysin and GAP-43 during the acute and latent phases of the lithium-pilocarpine model in the immature and adult rat. *Exp Neurol* 2007;204:720–32. <https://doi.org/10.1016/j.expneurol.2007.01.002>.

[73] Hayward NMEA, Ndode-Ekane XE, Kutchashvili N, Grohn O, Pitkanen A. Elevated cerebral blood flow and vascular density in the amygdala after status epilepticus in rats. *Neurosci Lett* 2010;484:39–42. <https://doi.org/10.1016/j.neulet.2010.08.013>.

[74] Joseph SA, Lynd-Balta E, O'Banion MK, Rappold PM, Daschner J, Allen A, et al. Enhanced cyclooxygenase-2 expression in olfactory-limbic forebrain following kainate-induced seizures. *Neuroscience* 2006;140:1051–65. <https://doi.org/10.1016/j.neuroscience.2006.02.075>.

[75] Jung K-H, Chu K, Lee S-T, Kim J-H, Kang K-M, Song E-C, et al. Region-specific plasticity in the epileptic rat brain: a hippocampal and extrahippocampal analysis. *Epilepsia* 2009;50:537–49. <https://doi.org/10.1111/j.1528-1167.2008.01718.x>.

[76] Kempainen S, Pitkanen A. Damage to the amygdalo-hippocampal projection in temporal lobe epilepsy: a tract-tracing study in chronic epileptic rats. *Neuroscience* 2004;126:485–501. <https://doi.org/10.1016/j.neuroscience.2004.03.015>.

[77] Kempainen EJS, Nissinen J, Pitkanen A. Fear conditioning is impaired in systemic kainic acid and amygdala-stimulation models of epilepsy. *Epilepsia* 2006;47: 820–9. <https://doi.org/10.1111/j.1528-1167.2006.00542.x>.

[78] Klitgaard H, Matagne A, Vanneste-Goemaere J, Margineanu D-G. Pilocarpine-induced epileptogenesis in the rat: impact of initial duration of status epilepticus on electrophysiological and neuropathological alterations. *Epilepsy Res* 2002;51: 93–107.

[79] Lehtimaki KA, Peltola J, Koskikallio E, Keranen T, Honkanen J. Expression of cytokines and cytokine receptors in the rat brain after kainic acid-induced seizures. *Brain Res Mol Brain Res* 2003;110:253–60.

[80] Leroy C, Roch C, Koning E, Namer J, Nehlig A. In the lithium-pilocarpine model of epilepsy, brain lesions are not linked to changes in blood-brain barrier permeability: an autoradiographic study in adult and developing rats. *Exp Neurol* 2003;182: 361–72.

[81] Lintunen M, Sallmen T, Karlstedt K, Panula P. Transient changes in the limbic histaminergic system after systemic kainic acid-induced seizures. *Neurobiol Dis* 2005; 20:155–69. <https://doi.org/10.1016/j.nbd.2005.02.007>.

[82] Liu S-J, Zheng P, Wright DK, Dezsö G, Braine E, Nguyen T, et al. Sodium selenate retards epileptogenesis in acquired epilepsy models reversing changes in protein phosphatase 2A and hyperphosphorylated tau. *Brain* 2016;139:1919–38. <https://doi.org/10.1093/brain/aww116>.

[83] Lurton D, Cavalheiro EA. Neuropeptide-Y immunoreactivity in the pilocarpine model of temporal lobe epilepsy. *Exp Brain Res* 1997;116:186–90.

[84] Motte J, Fernandes MJ, Baram TZ, Nehlig A. Spatial and temporal evolution of neuronal activation, stress and injury in lithium-pilocarpine seizures in adult rats. *Brain Res* 1998;793:61–72.

[85] Nakatsu Y, Kimura R, Handa J, Uemura S, Morikawa S, Inubushi T. Magnetic resonance imaging in status epilepticus elicited by kainate in rats. *Jpn J Psychiatry Neurol* 1993;47:406–7.

[86] Narkilahti S, Pirttilä TJ, Lukasiuk K, Tuunanen J, Pitkanen A. Expression and activation of caspase 3 following status epilepticus in the rat. *Eur J Neurosci* 2003;18: 1486–96.

[87] Nicoletti JN, Shah SK, McCloskey DP, Goodman JH, Elkady A, Atassi H, et al. Vascular endothelial growth factor is up-regulated after status epilepticus and protects against seizure-induced neuronal loss in hippocampus. *Neuroscience* 2008;151: 232–41. <https://doi.org/10.1016/j.neuroscience.2007.09.083>.

[88] Penschuck S, Bastlund JF, Jensen HS, Stensbol TB, Egebjerg J, Watson WP. Changes in KCNQ2 immunoreactivity in the amygdala in two rat models of temporal lobe epilepsy. *Brain Res Mol Brain Res* 2005;141:66–73. <https://doi.org/10.1016/j.molbrainres.2005.08.004>.

[89] Pereno GL, Beltramo CA. Timed changes of synaptic zinc, synaptophysin and MAP2 in medial extended amygdala of epileptic animals are suggestive of reactive neuroplasticity. *Brain Res* 2010;1328:130–8. <https://doi.org/10.1016/j.brainres.2010.01.087>.

[90] Pereno GL, Balaszczuk V, Beltramo CA. Kainic acid-induced early genes activation and neuronal death in the medial extended amygdala of rats. *Exp Toxicol Pathol* 2011;63:291–9. <https://doi.org/10.1016/j.etp.2010.02.001>.

[91] Perez-Cruz C, Rocha L. Kainic acid modifies mu-receptor binding in young, adult, and elderly rat brain. *Cell Mol Neurobiol* 2002;22:741–53.

[92] Pirttila TR, Pitkänen A, Tuunainen J, Kauppinen RA. Ex vivo MR microimaging of neuronal damage after kainate-induced status epilepticus in rat: correlation with quantitative histology. *Magn Reson Med* 2001;46:946–54.

[93] Pitkänen A, Tuunainen J, Halonen T. Vigabatrin and carbamazepine have different efficacies in the prevention of status epilepticus induced neuronal damage in the hippocampus and amygdala. *Epilepsy Res* 1996;24:29–45.

[94] Raffo E, Koning E, Nehlig A. Postnatal maturation of cytochrome oxidase and lactate dehydrogenase activity and age-dependent consequences of lithium-pilocarpine status epilepticus in the rat: a regional histochemistry study. *Pediatr Res* 2004;56:647–55. <https://doi.org/10.1203/01.PDR.0000139604.47609.8C>.

[95] Righini A, Pierpaoli C, Alger JR, Di Chiro G. Brain parenchyma apparent diffusion coefficient alterations associated with experimental complex partial status epilepticus. *Magn Reson Imaging* 1994;12:865–71.

[96] Roch C, Leroy C, Nehlig A, Namer IJ. Magnetic resonance imaging in the study of the lithium-pilocarpine model of temporal lobe epilepsy in adult rats. *Epilepsia* 2002;43:325–35.

[97] Sawamura A, Hashizume K, Yoshida K, Tanaka T. Kainic acid-induced substantia nigra seizure in rats: behavior, EEG and metabolism. *Brain Res* 2001;911:89–95.

[98] Scorz FA, Arida RM, Priel MR, Calderazzo L, Cavalheiro EA. Glucose utilization during status epilepticus in an epilepsy model induced by pilocarpine: a qualitative study. *Arq Neuropsiquiatr* 2002;60:198–203.

[99] Silva IR, Nehlig A, Rosim FE, Vignoli T, Persico DS, Ferrandon A, et al. The A1 receptor agonist R-Pia reduces the imbalance between cerebral glucose metabolism and blood flow during status epilepticus: could this mechanism be involved with neuroprotection? *Neurobiol Dis* 2011;41:169–76. <https://doi.org/10.1016/j.nbd.2010.09.004>.

[100] Su J, Yin J, Qin W, Sha S, Xu J, Jiang C. Role for pro-inflammatory cytokines in regulating expression of GABA transporter type 1 and 3 in specific brain regions of kainic acid-induced status epilepticus. *Neurochem Res* 2015;40:621–7. <https://doi.org/10.1007/s11064-014-1504-y>.

[101] Suleymanova EM, Gulyaev MV, Abbasova KR. Structural alterations in the rat brain and behavioral impairment after status epilepticus: an MRI study. *Neuroscience* 2016;315:79–90. <https://doi.org/10.1016/j.neuroscience.2015.11.061>.

[102] Tchekalarova J, Atanasova D, Nenchovska Z, Atanasova M, Kortenska L, Gesheva R, et al. Agomelatine protects against neuronal damage without preventing epileptogenesis in the kainate model of temporal lobe epilepsy. *Neurobiol Dis* 2017;104:1–14. <https://doi.org/10.1016/j.nbd.2017.04.017>.

[103] Tuunainen J, Lukasiuk K, Halonen T, Pitkänen A. Status epilepticus-induced neuronal damage in the rat amygdaloid complex: distribution, time-course and mechanisms. *Neuroscience* 1999;94:473–95.

[104] Tuunainen J, Halonen T, Pitkänen A. Status epilepticus causes selective regional damage and loss of GABAergic neurons in the rat amygdaloid complex. *Eur J Neurosci* 1996;8:2711–25.

[105] van Eijnsden P, Notenboom RGE, Wu O, de Graan PNE, van Nieuwenhuizen O, Nicolay K, et al. In vivo 1H magnetic resonance spectroscopy, T2-weighted and diffusion-weighted MRI during lithium-pilocarpine-induced status epilepticus in the rat. *Brain Res* 2004;1030:11–8. <https://doi.org/10.1016/j.brainres.2004.09.025>.

[106] van Vliet EA, Otte WM, Gorter JA, Dijkhuizen RM, Wadman WJ. Longitudinal assessment of blood-brain barrier leakage during epileptogenesis in rats. A quantitative MRI study. *Neurobiol Dis* 2014;63:74–84. <https://doi.org/10.1016/j.nbd.2013.11.019>.

[107] van Vliet EA, Otte WM, Wadman WJ, Aronica E, Kooij G, de Vries HE, et al. Blood-brain barrier leakage after status epilepticus in rapamycin-treated rats I: magnetic resonance imaging. *Epilepsia* 2016;57:59–69. <https://doi.org/10.1111/epi.13246>.

[108] Weise J, Engelhorn T, Dorfler A, Aker S, Bahr M, Hufnagel A. Expression time course and spatial distribution of activated caspase-3 after experimental status epilepticus: contribution of delayed neuronal cell death to seizure-induced neuronal injury. *Neurobiol Dis* 2005;18:582–90. <https://doi.org/10.1016/j.nbd.2004.10.025>.

[109] Wolf DC, Bueno-Junior LS, Lopes-Aguiar C, Do Val Da Silva RA, Kandratavicius L, Leite JP. The frequency of spontaneous seizures in rats correlates with alterations in sensorimotor gating, spatial working memory, and parvalbumin expression throughout limbic regions. *Neuroscience* 2016;312:86–98. <https://doi.org/10.1016/j.neuroscience.2015.11.008>.

[110] Yamada A, Momosaki S, Hosoi R, Abe K, Yamaguchi M, Inoue O. Glucose utilization in the brain during acute seizure is a useful biomarker for the evaluation of anticonvulsants: effect of methyl ethyl ketone in lithium-pilocarpine status epilepticus rats. *Nucl Med Biol* 2009;36:949–54. <https://doi.org/10.1016/j.nucmedbio.2009.06.008>.

[111] Yang J, He F, Meng Q, Sun Y, Wang W, Wang C. Inhibiting HIF-1alpha decreases expression of TNF-alpha and caspase-3 in specific brain regions exposed kainic acid-induced status epilepticus. *Cell Physiol Biochem* 2016;38:75–82. <https://doi.org/10.1159/000438610>.

[112] Sokoloff L, Reivich M, Kennedy C, Des Rosiers MH, Patlak CS, Pettigrew KD, et al. The [¹⁴C]deoxyglucose method for the measurement of local cerebral glucose utilization: theory, procedure, and normal values in the conscious and anesthetized albino rat. *J Neurochem* 1977;28:897–916.

[113] Fisher RS, Scharfman HE, deCurtis M. How can we identify ictal and interictal abnormal activity? *Adv Exp Med Biol* 2014;813:3–23. https://doi.org/10.1007/978-94-017-8914-1_1.

[114] Okuno H. Regulation and function of immediate-early genes in the brain: beyond neuronal activity markers. *Neurosci Res* 2011;69:175–86. <https://doi.org/10.1016/j.neures.2010.12.007>.

[115] Yang J, Ruchti E, Petit J-M, Jourdain P, Grenningloh G, Allaman I, et al. Lactate promotes plasticity gene expression by potentiating NMDA signaling in neurons. *Proc Natl Acad Sci U S A* 2014;111(33):12228. <https://doi.org/10.1073/pnas.1322912111>.

[116] Morgan JI, Cohen DR, Hempstead JL, Curran T. Mapping patterns of c-fos expression in the central nervous system after seizure. *Science* 1987;237:192–7. <https://doi.org/10.1126/science.3037702>.

[117] Shimada T, Takemoto T, Sugiura H, Yamagata K. Role of inflammatory mediators in the pathogenesis of epilepsy. *Mediators Inflamm* 2014;2014:901902. <https://doi.org/10.1155/2014/901902>.

[118] Choy M, Dube CM, Ehrengruber M, Baram TZ. Inflammatory processes, febrile seizures, and subsequent epileptogenesis. *Epilepsy Curr* 2014;14:15–22. <https://doi.org/10.5698/1535-7511-14.s2.15>.

[119] Ravizza T, Balosso S, Vezzani A. Inflammation and prevention of epileptogenesis. *Neurosci Lett* 2011;497:223–30. <https://doi.org/10.1016/j.neulet.2011.02.040>.

[120] Vezzani A, Moneta D, Richichi C, Aliprandi M, Burrows SJ, Ravizza T, et al. Functional role of inflammatory cytokines and antiinflammatory molecules in seizures and epileptogenesis. *Epilepsia* 2002;43(Suppl. 5):30–5.

[121] Schmued LC, Albertson C, Slikker WJ. Fluoro-Jade: a novel fluorochrome for the sensitive and reliable histochemical localization of neuronal degeneration. *Brain Res* 1997;751:37–46. [https://doi.org/10.1016/s0006-8993\(96\)01387-x](https://doi.org/10.1016/s0006-8993(96)01387-x).

[122] Castro OW, Furtado MA, Tilelli CQ, Fernandes A, Pajolla GP, Garcia-Cairasco N. Comparative neuroanatomical and temporal characterization of FluoroJade-positive neurodegeneration after status epilepticus induced by systemic and intrahippocampal pilocarpine in Wistar rats. *Brain Res* 2011;1374:43–55. <https://doi.org/10.1016/j.brainres.2010.12.012>.

[123] Imitola J, Raddassi K, Park KI, Mueller F-J, Nieto M, Teng YD, et al. Directed migration of neural stem cells to sites of CNS injury by the stromal cell-derived factor 1alpha/CXC chemokine receptor 4 pathway. *Proc Natl Acad Sci U S A* 2004;101:18117–22. <https://doi.org/10.1073/pnas.0408258102>.

[124] Nagao Y, Harada Y, Mukai T, Shimizu S, Okuda A, Fujimoto M, et al. Expressional analysis of the astrocytic Kir4.1 channel in a pilocarpine-induced temporal lobe epilepsy model. *Front Cell Neurosci* 2013;7:104. <https://doi.org/10.3389/fncel.2013.00104>.

[125] Garcia-Cairasco N. Puzzling challenges in contemporary neuroscience: insights from complexity and emergence in epileptogenic circuits. *Epilepsia Behav* 2009;14(Suppl. 1):54–63. <https://doi.org/10.1016/j.yebeh.2008.09.010>.

[126] Tejada J, Costa KM, Bertti P, Garcia-Cairasco N. The epilepsies: complex challenges needing complex solutions. *Epilepsia Behav* 2013;26:212–28. <https://doi.org/10.1016/j.yebeh.2012.09.029>.

[127] Reddy DS, Volkmer 2nd R. Neurocysticercosis as an infectious acquired epilepsy worldwide. *Seizure* 2017;52:176–81. <https://doi.org/10.1016/j.seizure.2017.10.004>.

[128] Neuberger Ej, Gupta A, Subramanian D, Korgaonkar AA, Santhakumar V. Converging early responses to brain injury pave the road to epileptogenesis. *J Neurosci Res* 2017. <https://doi.org/10.1002/jnr.24202>.

[129] Aronica E, Muhlebner A. Neuropathology of epilepsy. *Handb Clin Neurol* 2017;145:193–216. <https://doi.org/10.1016/B978-0-12-802395-2.00015-8>.

[130] Castro OW, Upadhyay D, Kodali M, Shetty AK. Resveratrol for easing status epilepticus induced brain injury, inflammation, epileptogenesis, and cognitive and memory dysfunction—are we there yet? *Front Neurol* 2017;8:603. <https://doi.org/10.3389/fneur.2017.00603>.

[131] Younus I, Reddy DS. Epigenetic interventions for epileptogenesis: a new frontier for curing epilepsy. *Pharmacol Ther* 2017;177:108–22. <https://doi.org/10.1016/j.pharmthera.2017.03.002>.

[132] Clossen BL, Reddy DS. Novel therapeutic approaches for disease-modification of epileptogenesis for curing epilepsy. *Biochim Biophys Acta Mol Basis Dis* 2017;1863:1519–38. <https://doi.org/10.1016/j.bbadiis.2017.02.003>.

[133] Italiano D, Striano P, Russo E, Leo A, Spina E, Zara F, et al. Genetics of reflex seizures and epilepsies in humans and animals. *Epilepsy Res* 2016;121:47–54. <https://doi.org/10.1016/j.eplepsyres.2016.01.010>.

[134] Kinjo ER, Rodriguez PXR, Dos Santos BA, Higa GSV, Ferraz MSA, Schmeltzer C, et al. New insights on temporal lobe epilepsy based on plasticity-related network changes and high-order statistics. *Mol Neurobiol* 2018;55:3990–8. <https://doi.org/10.1007/s12035-017-0623-2>.

[135] Webster KM, Sun M, Crack P, O'Brien TJ, Shultz SR, Semple BD. Inflammation in epileptogenesis after traumatic brain injury. *J Neuroinflammation* 2017;14:10. <https://doi.org/10.1186/s12974-016-0786-1>.

[136] Loscher W. Fit for purpose application of currently existing animal models in the discovery of novel epilepsy therapies. *Epilepsy Res* 2016;126:157–84. <https://doi.org/10.1016/j.eplepsyres.2016.05.016>.

[137] Tang F, Hartz AMS, Bauer B. Drug-resistant epilepsy: multiple hypotheses, few answers. *Front Neurol* 2017;8:301. <https://doi.org/10.3389/fneur.2017.00301>.

[138] Schulze-Bonhage A. A 2017 review of pharmacotherapy for treating focal epilepsy: where are we now and how will treatment develop? *Expert Opin Pharmacother* 2017;18:1845–53. <https://doi.org/10.1080/14656566.2017.1391788>.

[139] Araujo BHS, Torres LB, Guilhoto LMFF. Cerebral overinhibition could be the basis for the high prevalence of epilepsy in persons with Down syndrome. *Epilepsy Behav* 2015;53:120–5. <https://doi.org/10.1016/j.yebeh.2015.10.004>.

[140] Lothman EW, Bertram EH, Bekenstein JW, Perlin JB. Self-sustaining limbic status epilepticus induced by “continuous” hippocampal stimulation: electrographic and behavioral characteristics. *Epilepsy Res* 1989;3:107–19.

[141] Naylor DE. Glutamate and GABA in the balance: convergent pathways sustain seizures during status epilepticus. *Epilepsia* 2010;51(Suppl. 3):106–9. <https://doi.org/10.1111/j.1528-1167.2010.02622.x>.

[142] Soukupova M, Binaschi A, Falcicchia C, Palma E, Roncon P, Zucchini S, et al. Increased extracellular levels of glutamate in the hippocampus of chronically epileptic rats. *Neuroscience* 2015;301:246–53. <https://doi.org/10.1016/j.neuroscience.2015.06.013>.

[143] Mesulam MM. Neuroplasticity failure in Alzheimer's disease: bridging the gap between plaques and tangles. *Neuron* 1999;24:521–9.

[144] Sammons RP, Keck T. Adult plasticity and cortical reorganization after peripheral lesions. *Curr Opin Neurobiol* 2015;35:136–41. <https://doi.org/10.1016/j.conb.2015.08.004>.

[145] Altman J. Are new neurons formed in the brains of adult mammals? *Science* 1962;135:1127–8. <https://doi.org/10.1126/science.135.3509.1127>.

[146] Parent JM, Yu TW, Leibowitz RT, Geschwind DH, Sloviter RS, Lowenstein DH. Dentate granule cell neurogenesis is increased by seizures and contributes to aberrant network reorganization in the adult rat hippocampus. *J Neurosci* 1997;17:3727–38.

[147] Pierson MG, Swann J. Ontogenetic features of audiogenic seizure susceptibility induced in immature rats by noise. *Epilepsia* 1991;32:1–9.

[148] Sayin U, Hutchinson E, Meyerand ME, Sutula T. Age-dependent long-term structural and functional effects of early-life seizures: evidence for a hippocampal critical period influencing plasticity in adulthood. *Neuroscience* 2015;288:120–34. <https://doi.org/10.1016/j.neuroscience.2014.12.017>.

[149] Pitkänen A, Engel JJ. Past and present definitions of epileptogenesis and its biomarkers. *Neurotherapeutics* 2014;11:231–41. <https://doi.org/10.1007/s13311-014-0257-2>.

[150] Bauer S, van Alphen N, Becker A, Chiochetti A, Deichmann R, Deller T, et al. Personalized translational epilepsy research – novel approaches and future perspectives: part II: experimental and translational approaches. *Epilepsy Behav* 2017;76:7–12. <https://doi.org/10.1016/j.yebeh.2017.06.040>.

[151] Loscher W. Critical review of current animal models of seizures and epilepsy used in the discovery and development of new antiepileptic drugs. *Seizure* 2011;20:359–68. <https://doi.org/10.1016/j.seizure.2011.01.003>.

[152] Galanopoulou AS, Mowrey WB. Not all that glitters is gold: a guide to critical appraisal of animal drug trials in epilepsy. *Epilepsia Open* 2016;1:86–101. <https://doi.org/10.1002/epi4.12021>.

[153] Price JL. Comparative aspects of amygdala connectivity. *Ann N Y Acad Sci* 2003;985:50–8. <https://doi.org/10.1111/j.1749-6632.2003.tb07070.x>.

[154] Pitkänen A, Kemppainen S. Comparison of the distribution of calcium-binding proteins and intrinsic connectivity in the lateral nucleus of the rat, monkey, and human amygdala. *Pharmacol Biochem Behav* 2002;71:369–77. [https://doi.org/10.1016/s0091-3057\(01\)00690-6](https://doi.org/10.1016/s0091-3057(01)00690-6).

[155] Smith HR, Porrino LJ. The comparative distributions of the monoamine transporters in the rodent, monkey, and human amygdala. *Brain Struct Funct* 2008;213:73–91. <https://doi.org/10.1007/s00429-008-0176-2>.

[156] Chareyron LJ, Banta Lavenex P, Amaral DG, Lavenex P. Stereological analysis of the rat and monkey amygdala. *J Comp Neurol* 2011;519:3218–39. <https://doi.org/10.1002/cne.22677>.

[157] Kim MJ, Loucks RA, Palmer AL, Brown AC, Solomon KM, Marchante AN, et al. The structural and functional connectivity of the amygdala: from normal emotion to pathological anxiety. *Behav Brain Res* 2011;223:403–10. <https://doi.org/10.1016/j.bbr.2011.04.025>.

[158] Rosen JB, Donley MP. Animal studies of amygdala function in fear and uncertainty: relevance to human research. *Biol Psychol* 2006;73:49–60. <https://doi.org/10.1016/j.biopsych.2006.01.007>.

[159] Alvarez RP, Biggs A, Chen G, Pine DS, Grillon C. Contextual fear conditioning in humans: cortical–hippocampal and amygdala contributions. *J Neurosci* 2008;28:6211–9. <https://doi.org/10.1523/JNEUROSCI.1246-08.2008>.

[160] Morrison SE, Salzman CD. Re-valuing the amygdala. *Curr Opin Neurobiol* 2010;20:221–30. <https://doi.org/10.1016/j.conb.2010.02.007>.

[161] Coan AC, Morita ME, de Campos BM, Yasuda CL, Cendes F. Amygdala enlargement in patients with mesial temporal lobe epilepsy without hippocampal sclerosis. *Front Neurol* 2013;4:166. <https://doi.org/10.3389/fneur.2013.00166>.

[162] Kalviainen R, Salmenpera T, Partanen K, Vainio P, Riekkinen PS, Pitkänen A. MRI volumetry and T2 relaxometry of the amygdala in newly diagnosed and chronic temporal lobe epilepsy. *Epilepsy Res* 1997;28:39–50. [https://doi.org/10.1016/s0920-1211\(97\)00029-6](https://doi.org/10.1016/s0920-1211(97)00029-6).

[163] Bernasconi N, Bernasconi A, Caramanos Z, Antel SB, Andermann F, Arnold DL. Mesial temporal damage in temporal lobe epilepsy: a volumetric MRI study of the hippocampus, amygdala and parahippocampal region. *Brain* 2003;126:462–9. <https://doi.org/10.1093/brain/awg034>.

[164] Bonilha L, Kobayashi E, Rorden C, Cendes F, Li LM. Medial temporal lobe atrophy in patients with refractory temporal lobe epilepsy. *J Neurol Neurosurg Psychiatry* 2003;74:1627–30. <https://doi.org/10.1136/jnnp.74.12.1627>.

[165] Slomianka L, Amrein I, Knuesel I, Sorensen JC, Wolfer DP. Hippocampal pyramidal cells: the reemergence of cortical lamination. *Brain Struct Funct* 2011;216:301–17. <https://doi.org/10.1007/s00429-011-0322-0>.

[166] Pelkey KA, Chittajallu R, Craig MT, Tricoire L, Wester JC, McBain CJ. Hippocampal GABAergic inhibitory interneurons. *Physiol Rev* 2017;97:1619–747. <https://doi.org/10.1152/physrev.00007.2017>.

[167] Benoy A, Dasgupta A, Sajikumar S. Hippocampal area CA2: an emerging modulatory gateway in the hippocampal circuit. *Exp Brain Res* 2018;236:919–31. <https://doi.org/10.1007/s00221-018-5187-5>.

[168] Li Y, Mu Y, Gage FH. Development of neural circuits in the adult hippocampus. *Curr Top Dev Biol* 2009;87:149–74. [https://doi.org/10.1016/S0070-2153\(09\)01205-8](https://doi.org/10.1016/S0070-2153(09)01205-8).

[169] Pitkänen A, Savander V, LeDoux JE. Organization of intra-amygdaloid circuitries in the rat: an emerging framework for understanding functions of the amygdala. *Trends Neurosci* 1997;20:517–23.

[170] LeDoux J. The amygdala. *Curr Biol* 2007;17:R868–74. <https://doi.org/10.1016/j.cub.2007.08.005>.

[171] Swanson LW. Brain maps 4.0—structure of the rat brain: an open access atlas with global nervous system nomenclature ontology and flatmaps. *J Comp Neurol* 2018;526:935–43. <https://doi.org/10.1002/cne.24381>.

[172] Andersen ML, Winter LMF. Animal models in biological and biomedical research – experimental and ethical concerns. *An Acad Bras Cienc* 2019;91:e20170238. <https://doi.org/10.1590/0001-3765.20170238>.

[173] Lidster K, Jefferys JG, Blumcke I, Crunelli V, Flecknell P, Frenguelli BG, et al. Opportunities for improving animal welfare in rodent models of epilepsy and seizures. *J Neurosci Methods* 2016;260:2–25. <https://doi.org/10.1016/j.jneumeth.2015.09.007>.

[174] Bert B, Dorendahl A, Leich N, Vietze J, Steinfath M, Chmielewska J, et al. Rethinking 3R strategies: digging deeper into AnimalTestInfo promotes transparency in *in vivo* biomedical research. *PLoS Biol* 2017;15:e2003217. <https://doi.org/10.1371/journal.pbio.2003217>.